

AperTO - Archivio Istituzionale Open Access dell'Università di Torino

Centimetric circular areas uncolonized by microbial biofilms (CUMBs) on marble surfaces and insights on a lichen-related origin

This is a pre print version of the following article:

Original Citation:

Availability:

This version is available <http://hdl.handle.net/2318/1934672> since 2023-10-09T13:31:05Z

Published version:

DOI:10.1016/j.ibiod.2023.105681

Terms of use:

Open Access

Anyone can freely access the full text of works made available as "Open Access". Works made available under a Creative Commons license can be used according to the terms and conditions of said license. Use of all other works requires consent of the right holder (author or publisher) if not exempted from copyright protection by the applicable law.

(Article begins on next page)

1 **Centimetric circular areas Uncolonized by Microbial Biofilms (CUMBs) on marble**
2 **surfaces and insights on a lichen-related origin**

3 Marta Cicardi¹, Davide Bernasconi², Luca Martire², Linda Pastero², Giulia Caneva³, Sergio E.
4 Favero-Longo^{1,*}

5 ¹ Dipartimento di Scienze della Vita e Biologia dei Sistemi, Università di Torino, Viale
6 Mattioli 25, 10125 Torino, Italy; marta.cicardi@unito.it, sergio.favero@unito.it

7 ² Dipartimento di Scienze della Terra, Università di Torino, Via Valperga Caluso 35, 10125
8 Torino, Italy; davide.bernasconi@unito.it, luca.martire@unito.it, linda.pastero@unito.it

9 ³ Dipartimento di Scienze, Università di RomaTre, viale Marconi 446, 00146, Roma, Italy;
10 giulia.caneva@uniroma3.it

11

12 * Corresponding author

13 Sergio E. Favero Longo, PhD
14 Università degli Studi di Torino
15 Dipartimento di Scienze della Vita e Biologia dei Sistemi
16 Viale Mattioli 25, 10125 Torino, Italy
17 Tel. +390116705972
18 Fax +390116705962
19 sergio.favero@unito.it
20 orcid.org/0000-0001-7129-5975
21

23 **Abstract**

24 This study investigated the poorly known phenomenon of Centimetric circular areas
25 Uncolonized by Microbial Biofilms (CUMBs) which is frequently observed on natural and
26 heritage stone surfaces displaying widespread lithobiontic colonization. In order to unveil a
27 possible relationship with past lichen colonization, analyses were carried out on the
28 distribution, morphometry, physical and mineralogical properties, and microscopic features of
29 CUMBs on the marble surfaces of a balustrade in the Garden of a Savoy residence in Torino
30 (Italy; UNESCO-WHS 823bis) and in its original quarry site in the W-Alps. Image analyses
31 of CUMBs displayed a distributional and dimensional compatibility with lichen thalli (re-
32)colonizing surfaces in their vicinity. Invasive analyses on quarry materials displayed similar
33 microscopic modifications in marble layers beneath CUMBs and lichens, associated to a
34 higher stabilization of the calcite {01-12} form, which is favoured by the presence of organic
35 substances. These findings support the hypothesis of a lichen origin for some CUMBs, which
36 may derive from the modification of physical stone properties and/or a long-lasting
37 allelopathic effect affecting surface bioreceptivity.

38 **Keywords:** allelopathy; bioreceptivity; calcite reprecipitation; discolourations; lichen
39 secondary metabolites; stone cultural heritage

40

41 **1 Introduction**

42 Saxicolous lichens are common biodeteriogens of rocks, including the outdoor stone heritage
43 surfaces, and their occurrence and relevance in historical sites have been described since long
44 time (Nimis et al. 1992; Piervittori et al., 2004; Favero-Longo and Viles 2020). They usually
45 display an epilithic growth, with their thallus mostly developing on the stone surface and
46 some mycobiont structures penetrating the substrate. In other cases, however, they display an
47 endolithic growth, with the thallus (including the photobiont layer) growing entirely within
48 the rock substrate. Both these growth patterns are often associated with physical and chemical
49 deterioration processes (de los Rios and Souza Egipsy 2021; Pinna 2021). Physical
50 deterioration is mostly exerted by hyphal penetration and volume changes in cyclic hydration
51 and dehydration of thalli, which cause pressures and, as a consequence, disaggregation and
52 detachment of mineral grains (Chen et al. 2000; Salvadori and Casanova Municchia 2016).
53 Also, lichens secrete a huge variety of metabolites with acidic and chelating functions,
54 supporting chemical modification of rock-forming minerals and, sometimes, dissolution
55 processes (Seaward 2015; Gadd 2017). It is also proved that, at least in some cases,
56 respiration-induced acidification of the substrate is sufficient to solubilize minerals (Weber et
57 al. 2011).

58 Lichen colonization determines peculiar biodeterioration patterns on the rock surfaces, such
59 as pitting (formation of sub-millimetric cavities), exfoliations, and depressions (Lombardozi
60 et al. 2012; Pinna 2021), which may persist as tracks even after the life of thalli (Danin &
61 Caneva 1990; Caneva et al. 2020). Moreover, biomineral deposits (as oxalates) and traces of
62 secondary metabolites were recognized as markers of past colonization by lichens (Edwards
63 et al. 2003; Casanova-Municchia et al. 2014; Miralles et al. 2015). For some combinations of

64 species, lithologies, and climate conditions, however, macroscopic observations of differential
65 erosion with and without lichen thalli, as well as chemical analyses of substrate solubilization
66 rates, indicated that lichens can act as a physical barrier against other weathering factors and
67 pollutants (umbrella-like protective effect) (Carter and Viles 2005; McIlroy de la Rosa et al.
68 2014). It was also claimed that the precipitation of (bio-)minerals at the lichen-substrate
69 interface, as in the case of oxalate deposits, may produce a protective shield and reduce the
70 deterioration (Gadd and Dyer 2017). Other patterns of chemical transformation associated to
71 hyphal penetration may also seal and reduce the effective porosity of rock substrates,
72 contributing to a hardening and protective effect against abiotic weathering agents
73 (Guglielmin et al. 2011; Slavík et al. 2017).

74 It is worth noting that biodeterioration and bioprotection processes are not mutually exclusive,
75 and, in the case of a thallus on its substrate, they can counteract and/or combine their effects
76 (Bungartz et al. 2004; Bartoli et al. 2014; Morando et al. 2017). It is thus the dynamic balance
77 between biodeterioration and bioprotection functions that determines the final effect of a
78 certain lichen species on a certain lithology (McIlroy de la Rosa et al. 2013, 2014). However,
79 this also depends on the bioclimatic and (micro-)environmental conditions, with the same
80 species potentially providing bioprotection in wet temperate environments and
81 biodeterioration in hot dry ones (Carter and Viles 2005).

82 A differential biodeterioration of stone can occur not only depending on exposition, but also
83 in the same conditions, as observed in the S-facing exposure of the limestone walls of the
84 Church of the Virgin in Martvili (Georgia), where a differential erosion phenomenon started
85 with a circular discoloration was observed leading progressively to the detachment of flakes
86 of limestone at its center (Caneva et al. 2014). In such xeric conditions of the walls, the cause
87 was referred to an endolithic penetration of cyanobacteria and meristematic fungi, which
88 started the growth taking advantage from some endogenous discontinuities on the surfaces
89 (Caneva et al. 2014). Furthermore, more recently, on restored marble surfaces already
90 displaying advanced epilithic recolonization, a phenomenon of Centimetric circular areas
91 Uncolonized by Microbial Biofilms, totally or with circular uncolonized borders and only the
92 center colonized, was also described (Caneva et al. 2020). On the basis of historical
93 photographic documentation and additional literature-based clues, these areas were
94 hypothesized as tracks of past lichen colonization.

95 Indeed, such patterns of differential growths related to a different bioreceptivity (*sensu*
96 Guilitte 1995), that we propose to call CUMBs, are extremely widespread and visible in many
97 environmental contexts, both on rock outcrops and monuments, and on different stone
98 substrates, as marble, cement, sandstone and others (Fig. 1). In some cases, epilithic microbial
99 absence empirically appears related to microbial endolithic growths or inhibition haloes (Fig.
100 1A); see also Cuberos-Càceres et al. 2022), or to the inhibitory chemical effects of bird
101 excrements (Fig. 1B) or of some fruit dropping (Fig. 1C). In many others, the particular shape
102 of CUMBs, and co-presence of CUMBs and lichens in the present or in the past, may support
103 the hypothesis of a strict relationship among them (Figs. 1D-H).

104 Surprisingly, however, the phenomenon of CUMBs on stone surfaces, and particularly on
105 marble, has never been quantitatively characterized and, with respect to the lichen-related
106 origin, the processes involved are not yet clarified. In their work, Caneva et al. (2020)
107 suggested on a bibliographic basis that certain lichen species observed in the past on the
108 marble surfaces could have left long-lasting allelopathic substances, without excluding a

109 potential influence of lichen-induced modifications on rock physical properties. Both these
110 hypotheses, however, still need to be experimentally examined.

111 In this research, we aimed to verify the hypothesis that, at least in some cases, CUMBs on
112 marble surfaces are related to past interactions between the carbonate substrate and lichen
113 thalli, which may have determined physical modifications of the stone material and/or a long-
114 term allelopathic effect, affecting its bioreceptivity. In this effort to unveil a possible lichen
115 origin of some CUMBs, we will describe their distribution, morphometry, physical and
116 mineralogical properties, and microscopic features. To accomplish these goals, we examined
117 a marble balustrade in the Garden of a 17th century Residence of the Royal House of Savoy
118 (Villa della Regina, UNESCO-WHS 823bis, Torino, NW-Italy), deeply affected by lichen and
119 other lithobiotic recolonization, as well as by the CUMBs pattern, at approx. 20 years after
120 the last restoration intervention. Moreover, considering that in-depth modifications of marble
121 related to such phenomenon may be detectable only with destructive analyses, we also
122 collected samples from one of the original quarries in W-Alps. On both the heritage and
123 natural surfaces, CUMBs and their surrounding surfaces colonized by microbial biofilms were
124 characterized in terms of morphometry, color, water absorption and mineralogical
125 composition, by image analysis, colorimetry, contact sponge method and X-ray powder
126 diffraction, respectively. For natural surfaces, the occurrence of biological structures and
127 other characterizing features beneath the colonized and uncolonized rock surfaces was also
128 evaluated by light, fluorescence and cathodoluminescence microscopy. Each analysis was
129 also carried out on nearby areas currently colonized by lichens, as a comparison.

130

131 **2 Materials and methods**

132 *2.1 Study sites*

133 The CUMB phenomenon and lichen colonization were investigated at (a) the Villa della
134 Regina (Torino, Italy; UTM ED50 32T 45°03'28.93"N 7°42'28.78"E; 300 m a.s.l.) and (b) the
135 marble quarry of Rocca Bianca (Prali, Germanasca Valley, Torino, Italy; UTM ED50 32T
136 44°54'24"N 7°04'58"E; 1943 m a.s.l.).

137 The Villa della Regina is located on the Western side of the Hill of Torino, at 1.2 Km from
138 the Po River and 2.4 Km from the city center, lying in the Cfa climatic zone (C – temperate, f
139 - no dry season a - hot summer, according to the Köppen Geiger climate classification; Kottek
140 et al. 2006), with average temperatures ranging from 2.5°C (av. min. December) to 27.9°C
141 (av. max. July) and average annual rainfall around 870 mm
142 (https://webgis.arpa.piemonte.it/secure_apps/portale-sul-clima-in-piemonte/). The buildings
143 are surrounded by different gardens, which include various architectural elements, like
144 fountains, statues, grottos, and balustrades. Here, we focused the investigations on the sun-
145 exposed, upper horizontal surfaces of the capstones of the first balustrade upwards the main
146 building (Fig. 2A), limiting the western side of the Garden of Flowers, structured in two
147 branches (northern and southern). Each branch, consisting of a straight and a curved part,
148 includes six and three modules (approx. 3.6 × 0.3 m), respectively, of columnar balusters
149 covered by a capstone and delimited by two pillars. The balustrade was severely damaged
150 during second world war and, thus, partially reassembled in early 1950s. Before the public
151 opening of the Villa in 2007, after decades of abandonment, stone surfaces of the Garden
152 underwent restoration, including the examined balustrade in summer 2003. The main capstone

153 materials of the balustrade are two marbles quarried in W-Alps, widely used in historical
154 buildings and monuments in Torino, namely the marble of Prali and the marble of Brossasco.
155 Both are (between others) part of the Palaeozoic marbles belonging to the Dora Maira
156 geological unit (Borghi et al. 2014).

157 The quarry of Rocca Bianca is located on the NW side of the homonymous mountain, lying in
158 the Dfc zone (D-continentale, f-no dry season, c-cold summer; data quantified in the closest
159 monitoring station of Prali, at 1385 m a.s.l.: average temperature ranging from -5.0°C to
160 15.0°C, average annual rainfall around 1400 mm
161 (<https://nomadseason.com/climate/italy/piedmont/prali.html>). It was the first, historic site of
162 extraction of the marble of Prali, which is perfectly white and composed by medium-grained
163 (0.1-0.8 mm) calcite (95%) with grey veins of mica and chlorite crystals (Borghi et al. 2014;
164 Marini and Mossetti 2006). At present, it has been abandoned for several decades, but still
165 displays extractive walls and quarried blocks, together with ruined buildings and natural
166 outcrops. In the quarry, the marble forms several transposed layers (up to a few metres thick)
167 embedded within micaschists and is characterized by dominant white(-grey) levels alternating
168 with centimetre-thick green dolomite-rich levels (Ghelli 2004). Investigations particularly
169 focused on six, sun-exposed decimetric to metric blocks differing for inclination and lichen
170 community (Fig. 2D-I; blocks 1-6).

171 *2.2. Survey of lithobiontic colonization*

172 Surveys of lichen diversity were carried out on the balustrade of Villa della Regina and in the
173 quarry, finalized to detect dominant species. Lichens were identified on the basis of the online
174 keys published in ITALIC, the Information System of the Italian Lichens, version 07 (see
175 Nimis & Martellos 2020), accessed in autumn 2022. TLC analyses of the secondary
176 metabolites in some thalli followed Orange et al. (2001). Nomenclature of species follows
177 Nimis (2022).

178 Biofilms surrounding the CUMBs were also preliminary investigated with regard to their
179 main lithobiontic components, by microscopy observations under a Nikon Eclipse E400.

180 *2.3 Surveys and morphometric characterization of the CUMBs*

181 CUMBs on the balustrade of Villa della Regina were surveyed using an image-analysis
182 approach, particularly focusing on those with diameter higher than 1.5 cm because of their
183 clearly distinguishable appearance at distance. In particular, 6 and 5 capstones were selected
184 for the curved and straight branches of the balustrade, respectively, that is one capstone every
185 three for the curved branch and one every two for the straight one. Digital images (800dpi)
186 were collected using a scanner Epson V10 and the program Epson Scan. They were analyzed
187 by the software WinCam Pro2007d (Regent's Instrument), which quantifies pixels on the
188 basis of color or gray levels, allowing to define the presence and dimension of CUMBs (and
189 lichen thalli), following the protocol proposed by Gazzano et al. (2009). CUMB diameters (or
190 main axis, in the case of non-circular shapes) and circularity were then measured with the
191 program ImageJ (v. 1.46r), operating on the pixel classification image produced by WinCam
192 (Fig. S1).

193 The same protocol, but images acquired with a Canon EOS 750D, was used to examine
194 CUMBs (and lichen thalli) on the blocks of the abandoned quarry of Rocca Bianca.

195 A dimensional analysis of lichen thalli was performed for both the sites following the protocol
196 adopted for CUMBs. Dimensions of thalli and CUMBs were compared by means of ANOVA

197 with post-hoc Tukey's test to detect the matrix of pairwise comparison probabilities, using
198 Systat 10.2 (Systat Software Inc., San Jose, CA).

199 *2.4 Physical and mineralogical characterization of the CUMBs*

200 2.4.1 Colorimetric analysis

201 Colorimetric analyses of CUMBs, and their surrounding surfaces colonized by microbial
202 biofilms, were carried out on the balustrade and on blocks of the quarry of Rocca Bianca. For
203 each of 120 randomly selected CUMBs on the balustrade, from 1 to 5 measures were
204 collected depending on the CUMB size, together with an equal number of measures from the
205 surrounding surfaces (in total, 425 measures distributed on the 11 selected capstones). With
206 the same approach, a total of 213 measures were collected in the quarry.

207 Colorimetric measurements were carried out by a portable spectrophotometer (Konica
208 Minolta CM-23d), under the following conditions: geometrical condition d/8 specular
209 component included, D65 illuminant, 2° observer, target area of 8 mm diameter. The data
210 were analyzed by the CIELAB color system (ISO/CIE 2019), evaluating each color by three
211 cartesian or scalar coordinates: L* (lightness, 0-100 black - white); a* (red - green); b*
212 (yellow - blue).

213 For each group of measures (i.e. CUMB and its colonized surrounding), a ΔE^*_{ab} value was
214 calculated by comparing the average measure obtained on the CUMB with that obtained on
215 the surrounding surfaces colonized by the biofilm (formula 1).

$$216 (1) \Delta E^*_{ab} = [(\bar{L}_C - \bar{L}_B^*)^2 + (\bar{a}_C - \bar{a}_B^*)^2 + (\bar{b}_C - \bar{b}_B^*)^2]^{1/2}$$

217 Where:

218 C = CUMB

219 B = biofilm colonized surfaces

220 To visualize the L_{ab}^* coordinates on a bidimensional plane, a plan (x; y) with the values (L*;
221 a*/b*) was created.

222 2.4.2 Water absorption analysis

223 The water absorption (W_a) beneath CUMBs and the surrounding biofilm was evaluated using
224 the contact sponge method, standardized by CEN (EN 17655, 2021). It requires the adoption
225 of a 1034 Rodac plate (23.76 cm²) containing a natural fiber Calypso sponge produced by
226 Spontex that was imbibed with water to become thicker than the rim of the plate. The sponge
227 was pressed on the stone surface for 1 minute and the water absorption was determined by
228 calculating the difference, in mg/cm², between the sponge weights measured before and after
229 the contact with the surface (ΔW_a).

230 In the case of the balustrade, six couple of measurements were carried out in CUMBs (ΔW_{a-}
231 $CUMB$) and surrounding colonized areas (W_{a-bio}). In the case of the samples from the quarry of
232 Rocca Bianca, CUMB areas were generally too small to adopt the sponges specifically sold
233 for this test. Accordingly, a natural fiber Calypso sponge produced by Spontex was cut to
234 enter in a cap of a jar with an area of 7.54 cm² and pressed on the CUMBs surface for 1
235 minute. Twelves couples of spot measurements were carried out on CUMBs (ΔW_{a-CUMB}) and
236 in the colonized nearby areas (W_{a-bio}), considered both before and after a gentle cleaning by
237 brush. The difference in water absorption per each couple of measures obtained on the
238 balustrade and the quarry blocks was finally expressed as $\Delta W_{a-CUMB}/W_{a-bio}$ ratio.

239 2.4.3 X-ray powder diffraction analysis

240 X-ray powder diffraction (XRPD) analyses were performed on sets of samples scraped from
241 randomly selected CUMBs on the balustrade (n=4) and the quarry blocks (n=15; block 1,
242 n=3; block 2, n=3; block 5, n=6; block 6, n=3), their surrounding surfaces colonized by
243 biofilms and/or lichens, and (in the case of the quarry blocks) underneath freshly cut surfaces.
244 In particular, analyses on the balustrade considered the epilithic lichens *Circinaria* gr.
245 *calcareo* (L.) A. Nordin, Savić & Tibell and *Verrucaria macrostoma* DC, and those on the
246 quarry considered the epilithic *Staurothele areolata* (Ach.) Lettau and the endolithic
247 *Pyrenodesmia erodens* (Tretiach, Pinna & Grube) Søchting, Arup & Frödén and *Thelidium*
248 *incavatum* Mudd. The XRPD patterns were acquired with a Miniflex 600 diffractometer
249 (Rigaku, Tokyo, Japan) operating at 40 kV and 15 mA, using Cu-K α radiation ($\lambda = 1.5406 \text{ \AA}$),
250 in the 2θ range of 3° to 70° , scan speed $2^\circ/\text{min}$ with step size 0.02° . Qualitative and
251 semiquantitative analyses were performed with SmartLab Studio II version 4.3 (Rigaku),
252 using database PDF-4/Minerals 2020, to recognize main phases and peak heights referring to
253 their different crystallographic planes. For each XRPD pattern, the peak height (I, counts) and
254 the full-width at half maximum (FWHM, $^\circ$) were determined for the main {10–14} and the
255 less intense {01-12} peaks of calcite. In the case of the balustrade, ratios $(I/\text{FWHM})_{\text{Cal } 01-12}$ /
256 $(I/\text{FWHM})_{\text{Cal } 10-14}$ calculated for CUMBs and lichens were compared with those obtained
257 for the biofilm colonized surfaces (formula 2).

$$258 \quad (2) \quad \Delta\% \{01 - 12\}_{\text{balustrade}} = \frac{\beta_{C,L}}{\beta_{\text{biofilm}}}$$

259 Where:

$$260 \quad \beta = \frac{(I/\text{FWHM})_{\text{Cal } 01-12}}{(I/\text{FWHM})_{\text{Cal } 10-14}}$$

261 C = CUMB

262 L = lichen colonized surfaces.

263

264 In the case of the quarry blocks, ratios $(I/\text{FWHM})_{\text{Cal } 01-12}/(I/\text{FWHM})_{\text{Cal } 10-14}$ calculated for
265 CUMBs, lichen and biofilm colonized surfaces were compared with those obtained for the
266 fresh, unexposed rock volumes (formula 3).

$$267 \quad (3) \quad \Delta\% \{01 - 12\}_{\text{block } n} = \frac{\beta_{C,L,B}}{\beta_{\text{unexposed rock}}}$$

268 Where:

269 block n = quarry blocks 1-6

$$270 \quad \beta = \frac{(I/\text{FWHM})_{\text{Cal } 01-12}}{(I/\text{FWHM})_{\text{Cal } 10-14}}$$

271 C = CUMB

272 L = lichen colonized surfaces

273 B = biofilm colonized surfaces

274

275 2.5 UV and microscopic observations of internal stone features

276 Microscopic observations of cross sections were carried out to investigate the growth of
277 lichens and biofilms within the six blocks of Rocca Bianca, as well as the presence of organic
278 substances in general, and to compare the observed patterns with those detected beneath
279 CUMBs. To accomplish this goal, marble samples of heterogeneous dimensions (l×w×d: 3-
280 40×3-30×0.5-20 cm) were collected, including lichens and/or CUMBs. Their natural surfaces
281 and those freshly broken by hammer were preliminary observed under long (365 nm) wave
282 UV using a fluorescence analysis cabinet (Model CM-10; Spectroline, Westbury, NY), which
283 could give preliminary insights on the presence of organic substance (Tyson 2012).

284 A total of 14 polished cross sections were prepared from the blocks, freshly cut with a
285 diamond disk saw. A first set of observations was conducted under optical microscopy in
286 visible light and epifluorescence, using a Nikon Eclipse E400 equipped with two filter blocks,
287 namely, UV-2A (ex 330-380 nm, dm 400, ba 420) and B-2A (ex 450-490, dm 505, ba 520),
288 and a digital camera. Thereafter, the sections were stained with the Periodic acid Schiff's
289 method (Whitlach and Johnson, 1974), that colours polysaccharides (chitin in the case of the
290 mycobiont partner) inside the stone in shades of magenta, and were observed under a
291 stereomicroscope Olympus SZH. The following parameters were evaluated and quantified:
292 presence and depth of massive hyphal penetration component (i.e. the depth to which hyphae
293 continuously penetrate through intragranular and intergranular voids beneath the
294 whole surface extension of the thallus; *sensu* Favero-Longo et al. 2005, 2009; HD),
295 presence of endolithic biological structures, stained by PAS, not related to a surface
296 lithobiontic cover (deep growths, DG), presence and thickness of a white opalescent layer
297 (WL), presence and thickness of a dark layer (DL), fluorescence phenomena in the whitish
298 (WF), orange (OF), pink (PF), yellow (YF) and blue (BF) chromatic range. For five selected
299 sections, corresponding thin cross-sections were prepared to run petrographic observations.
300 These were observed using a polarizing microscope equipped with a cathodoluminescence
301 system CITL 8200 mk3 (operating conditions of about 17 kV and 400 µA) in order to search
302 for the potential presence of calcite phases of different origin (Machel, 2000) at the lichen-
303 marble interfaces and in correspondence of the CUMBs.

304 The results of UV and microscopic observations were finally visualized using a principal
305 coordinate analysis (PCoA) plot (symmetric scaling, centring samples by samples, centring
306 species by species, performed using CANOCO 4.5; Ter Braak & Smilauer, 2002).

307

308 **3 Results**

309 *3.1 Distribution and morphometry of CUMBs on the marble balustrade and quarried blocks,* 310 *in comparison with lichens*

311 Image analysis of the marble capstones at the Villa della Regina visualized a total of 960
312 CUMBs, with a main axis higher than 1.5 cm, that is approx. 80 CUMBs per square meter
313 (Fig. 2A). These were surrounded by a widespread dark microbial biofilm, mainly composed
314 of cyanobacteria and microcolonial fungi (Fig. S2A), and, subordinately, by epilithic crustose
315 lichens, including species with continuous centimetric thalli (*Circinaria* gr. *calcarea* and
316 *Verrucaria macrostoma*) (Fig. 2B,C) and others of lower, (sub-)millimetric dimensions (Table
317 S1). Some of these thalli were locally bordered by biofilm free areas (Fig. S3), which
318 sometimes extended in the direction of water washout (Fig. 2C). It is worth noting that
319 *Circinaria* samples from the balustrade were morphologically identifiable as *C. gr. calcarea*
320 (asci with 4 spores, sub-globose, 24×22 µm; cortex, medulla and apothecium K-; medulla I-),

321 but, on the basis of TLC, they lacked aspicilin. As expected, *V. nigrescens* did not exhibit
322 lichen secondary metabolites.

323 Image analysis showed that CUMBs on the balustrade had a major axis in the range 1.7-8.2
324 cm (Fig. 3A), with highest frequency of CUMBs with major axis between 2.0 and 4.0 cm
325 (51%; dispersion of data detailed in Fig. S4). The median circularity (ratio of the main axes)
326 of CUMBs was 1.3 (central quartiles comprised between 1.1 and 1.6; 5-95 percentiles
327 between 1.0 and 2.9), indicating a rather circular size (Fig. 3C). With respect to the lichen
328 thalli, the median major axis, and the circularity ratio of *C. gr. calcarea* were 2.2 cm and 1.2,
329 respectively, while in the case of *V. macrostoma* they were 1.1 cm and 1.3, respectively.
330 *Candelariella aurella* (Hoffm.) Zahlbr. and *Myriolecis gr. dispersa* (Pers.) Sliwa, Zhao Xin &
331 Lumbsch were widespread on the balustrade, and *Xanthocarpia crenulatella* (Nyl.) Frödén,
332 Arup & Søchting locally occurred, but they all displayed small thalli (av. main axis <0.5 cm).

333 The survey in the quarry of Rocca Bianca similarly showed marble surfaces displaying co-
334 presence of microbial biofilm (Fig. S2B), CUMBs and lichens (blocks 1-5; Fig. 2D-H), and
335 also a block, free of lichens, with CUMBs with uncolonized circular borders and the
336 colonized center, similar to those described by Caneva *et al.* (2020) (block 6; Fig. 2I). Lichen
337 communities associated with the CUMBs on the different examined blocks included epilithic
338 crustose species of genera *Staurothele* and *Calogaya*, and endolithic species of genera
339 *Thelidium* and *Pyrenodesmia* (Table S1, with details on the different blocks). On these blocks,
340 a total of 680 CUMBs was quantified. Their frequency was strongly different on the different
341 blocks, ranging between approx. 70 (block 1a) to 0.5 (blocks 3 and 6) per square decimeter,
342 and was significantly proportional to the number of lichen thalli on the same surfaces
343 ($R^2=0.91$; $p<0.01$; Fig. S5). The species of the family Verrucariaceae observed on the
344 examined marble surfaces lack lichen secondary metabolites, while, in the case of
345 Teloschistaceae, the epilithic *Calogaya pusilla* (A. Massal.) Arup, Frödén & Søchting
346 produces antraquinones and the endolithic *P. erodens* produces *Sedifolia*-grey pigments.

347 Measures of CUMBs and associated lichens in the quarry of Rocca Bianca are separately
348 reported for the examined blocks (Fig. 3B). On blocks 1-2-4-5, the dimensional range of
349 CUMBs and lichens partially overlapped, with the former being always slightly, but
350 significantly wider, while CUMBs were strongly wider than lichens on block 3. On blocks 1a-
351 d, 2, and 3 (Fig. 2D-F), CUMBs with main axis ranging from av. 0.7 to 3.2 cm were placed
352 between distinct thalli of *Staurothele areolata* (Ach.) Lettau with diameters of av. 0.6-0.7 cm
353 (blocks 1, Fig. 2D; block 3, Fig. 2F) or contiguous ones, determining a continuous
354 pluricentimetric colonization (block 2, Fig. 2E). Some thalli of irregular shape due to a partial
355 detachment of areolae made visible the substrate (Fig. 2Da), and or were surrounded by
356 uncolonized circular borders (Fig. 2F), with patterns resembling that of the adjacent CUMBs.
357 CUMBs and lichens also coexisted on blocks 4 and 5, characterized by epilithic thalli of
358 *Calogaya pusilla* and endolithic thalli of *Thelidium incavatum* and *Pyrenodesmia erodens*,
359 with 5-95 percentiles between 0.3-1.8 cm, observed both surrounded by a dark microbial
360 biofilm and in the middle of CUMBs (Fig. 2G-H). On blocks 1, 2, 4 and 5, the circularity of
361 CUMBs did not significantly differ from that of lichen, while it was lower in the case of block
362 3 (Fig. 3D). Few larger CUMBs, with an average main axis of 6 cm were observed on the
363 vertical surface of block 6, covered by a dark microbial biofilm for the rest and free of lichens
364 (Fig. 2I). These CUMBs were peculiarly colonized by the biofilm in their central part.

365 *3.2 Physical modifications of the stone material in CUMBs and mineralogical investigation*

366 The colorimetric analysis of the CUMBs on the balustrade quantified the colour difference
367 with respect to the nearby biofilm-colonized areas ($\Delta E^*_{ab} 20.11 \pm 1.77$), and data showed that
368 this was due to a difference in Lightness (L^*), while a^*/b^* ratio was similar (Fig. 4A). In
369 particular, L^* was significantly lower in the case of surfaces colonized by the microbial
370 biofilm. A similar pattern of L^* values was quantified at the Rocca Bianca quarry, where the
371 fresh cut stone showed even higher values than the CUMBs and a slightly lower a^*/b^* ratio
372 (due to slightly higher b^* values; not shown), although shifts were minimal (Fig. 4B).

373 CUMBs displayed a lower absorption with respect to the nearby areas covered by the biofilm,
374 on both the balustrade (median $\Delta W_{a-CUMB}/W_{a-bio} = 0.75$, with 5-95 percentiles in the range
375 0.55-0.85) and the blocks sampled from the quarry of Rocca Bianca (median $W_{a-CUMB}/W_{a-bio} =$
376 0.8 with 5-95 percentiles in the range 0.5-0.9) (Fig. 5). In the case of these latter, however, the
377 ratio was inverted when the measures were repeated after the biofilm removal (median W_{a-}
378 $CUMB}/W_{a-bio} = 1.4$ with 5-95 percentiles in the range 1.05-2.1).

379 X-ray diffraction of balustrade samples showed some higher presence of calcite with
380 stabilization of the calcite {01-12} form in correspondence of CUMBs with respect to the
381 nearby areas colonized by biofilms. In Fig. 6A, such pattern is shown by positive values of
382 percentage difference (+45%) between the $(I/WHM)_{Cal\ 01-12}/(I/WHM)_{Cal\ 10-14}$ ratios
383 calculated for the CUMBs and the nearby areas colonized by biofilms. Such positive
384 percentage difference was also detected (+55%) by comparing samples collected beneath *C.*
385 *calcareea* with the biofilm colonized areas (Fig. S6), while similar $(I/WHM)_{Cal\ 01-}$
386 $12}/(I/WHM)_{Cal\ 10-14}$ ratios were displayed by *V. macrostoma* and the biofilm.

387 In the case of samples from the quarry, $(I/WHM)_{Cal\ 01-12}/(I/WHM)_{Cal\ 10-14}$ calculated for
388 each block for CUMBs, biofilms and/or lichens were compared with those obtained for fresh
389 unexposed volumes (Fig. 6B). CUMBs on blocks 6 and 1 displayed relatively higher
390 percentage differences (av. approx. +500% and +200%) with respect to the fresh controls in
391 comparison with the biofilm (+50%) and *Staurothele areolata* (+400%), respectively. In the
392 case of block 5, CUMBs and *P. erodens* displayed positive percentage differences (approx.
393 +50%) of $(I/WHM)_{Cal\ 01-12}/(I/WHM)_{Cal\ 10-14}$ ratios with respect to the fresh control, while *T.*
394 *incavatum* displayed similar values. Only in the case of block 2, a negative percentage
395 difference of $(I/WHM)_{Cal\ 01-12}/(I/WHM)_{Cal\ 10-14}$ ratios was observed with respect to fresh
396 controls for both the CUMBs and the large thalli of *S. areolata*.

397 Oxalates were not found in correspondence of any CUMB, but only beneath *Circinaria* thalli
398 on the balustrade.

399 3.3 Stone features and biological structures beneath CUMBs, in comparison with biofilms 400 and lichens

401 The marble samples collected in the quarry and observed under UV light and by fluorescence
402 microscopy displayed remarkable autofluorescence phenomena both at their surface and the
403 (sub-)millimetric layers beneath it, exposed in the polished cross sections. Besides the
404 chlorophyll red autofluorescence, associated to epilithic and endolithic lichen photobionts and
405 some phototrophic components of biofilms, orange, pinkish-orange, yellow, and whitish
406 autofluorescence's were observed in correspondence of both CUMBs and/or nearby colonized
407 areas, although clear patterns were hardly recognizable. In particular, orange fluorescence was
408 observed on the surface and in the depth (down to 5mm) of block 6, in correspondence of the
409 biofilm surrounding the CUMBs (Fig. S7A), while these latter did not show the same pattern

410 (Fig. S7C). Whitish, pinkish-orange and yellowish fluorescence -extended from the surface to
411 the upper layers of the rock- characterized CUMBs interposed between the grey endolithic
412 thalli of *P. erodens* and *T. incavatum* on blocks 5 (Fig. S7E), and in the proximity of thalli of
413 *C. pusilla* and the biofilm on block 4, respectively. On blocks 1, pinkish fluorescence
414 characterized some, but not all, CUMBs and thalli of *S. areolata* (Fig. S7G), which were not
415 associated to fluorescence phenomena on block 2.

416 PAS staining of the cross sections, representative of the different quarry blocks, did not stain
417 the CUMBs surfaces and did not visualize any remarkable penetration of biological structures
418 beneath them. Except for blocks 3 and 4, an uncolonized, white opalescent layer from the
419 CUMB surface down to 0.5-3.0 mm was a common trait (Fig. S7D). Only in some cases, a
420 dark band (block 6) and/or deep hyphal growths (blocks 1, 2, 5, 6) were observed beneath this
421 opalescent layer. Microscopical observation of the colonized areas surrounding the CUMBs
422 displayed microbial growth from the surface down to a depth of 6 mm. In some samples, a
423 dark band was also observed at this depth (Fig. S7B). The white opalescent layer was
424 observed with a lower frequency beneath the biofilm of block 6 and also of block 4, where it
425 was not present beneath the CUMBs.

426 All lichens exhibited a hyphal penetration component developing within the rock, but with
427 different spread and depth depending on the species. *P. erodens* displayed pervasive hyphal
428 penetration within small channels perpendicular to the surface down to 0.3 mm, with thin
429 hyphae locally extending to higher depths, down to 5.5 mm (Fig. S7F). *T. incavatum*
430 massively penetrated the marble down to 0.5 mm, with a sparse penetration of thin hyphae
431 being locally observed down to 1.3 mm. The epilithic *S. areolata* showed a pervasive
432 penetration in the case of large thalli on blocks 2 and 3, with hyphal bundles widespread
433 within the mineral substrate down to 2.0 mm, and thin hyphae diffusely penetrating down to
434 8.0 mm. The smaller thalli of the same species on block 1 only displayed a similar network of
435 thin hyphae, penetrating down to a maximum of 5.7 mm (Fig. S7H). A white opalescent layer,
436 similar to that observed beneath CUMBs, was observed immediately beneath the endolithic
437 thalli on block 5 and *S. areolata* on blocks 1, 2 and 3. A darker band parallel to the surface
438 was also observed in the case of blocks 2, 3 (large thalli of *S. areolata*) and 5 (*P. erodens*).

439 In all cases, cathodoluminescence microscopy observation on thin cross sections obtained
440 from the same blocks observed under fluorescence and light microscopy (and examined with
441 XRPD) did not detect differences in surface and deep rock layers, including those displaying
442 the various fluorescence phenomena, potentially informative on calcite phases of different
443 origin (Fig.S8).

444 The PCoA, which extracted four main axes explaining 97.5% of total variance, summarizes in
445 Fig. 7 the variability registered by the UV and microscopic observations. Hyphal penetration
446 depth (HD), dark layer thickness (DL) and orange fluorescence (OF) were positively related
447 to the first (46.9% of total variance), second (29.4%) and third (14.0%) axes, respectively.
448 Deep growths (DG, that is the presence of PAS-stained structures beginning only from deep
449 layers) was negatively correlated to the first axis, while white layer (WL) and whitish
450 fluorescence (WF) showed negative correlations with all the three axes. Most of CUMBs
451 clustered in the third quadrant, positively related to DG and WL, although some of them also
452 scattered along the second axis, related to DL. *S. areolata* and *P. erodens* mostly scattered in
453 the lower quadrants, displaying higher positive correlation with HD than *T. incavatum*. This
454 latter mostly scattered in the left side of the diagram, showing a high correlation with both

455 WF and WL along the third axis. Biofilm samples were heterogeneously distributed along the
456 first axis, in some cases showing positive correlation with the DL and the OF along the
457 second and third axes, respectively. Yellow, pink and blue fluorescence (YF, PF, BF) were
458 superimposed in the third quadrant oppositely to HD and DL, likely driven by their limited
459 number of reports. Although some clustering of samples obtained from each block was
460 detected, this appeared subordinate to the described patterns related to different lithobionts
461 and CUMBs.

462

463 **4 Discussion**

464 At the best of our knowledge, glossaries internationally accepted as official references in the
465 framework of Cultural Heritage conservation (e.g., Vergès-Belmin, 2008) do not include any
466 dedicated term and description for the centimetric circular areas persistently free from
467 epilithic microbial growths, that we examined here under the term of CUMBs. As previously
468 shown, they can be the case of absence of natural colonization (as in the quarry) or
469 recolonization following restoration interventions (as for the Villa della Regina). Although
470 colorimetric results (Fig. 4) may qualify CUMBs as discolorations (i.e. changes of rock
471 colour, *sensu* Vergès-Belmin, 2008), they result from the absence of a surrounding microbial
472 deterioration pattern, and may even represent bioprotection features. Nevertheless, their
473 characterization and that of the causes of these differential bioreceptivity patterns appear
474 worth to be considered. Their relevance arises not only for the need of better qualify the visual
475 features of stone surfaces, giving useful nomenclatures for communication issue, but also for
476 the potential clue to address innovative strategies to avoid recolonization processes following
477 restoration.

478 In this work, we provided a first morphometric characterization of CUMBs on a marble, and
479 we verified their distributional and dimensional compatibility with lichens (re-)colonizing
480 surfaces in their vicinity, both on a heritage structure and in the original quarry site, now
481 representing a semi-natural condition. Moreover, invasive analyses on quarry materials
482 displayed, for marble layers immediately beneath CUMBs and lithobionts, several modified
483 patterns with respect to the fresh rock, including chromatic shifts and fluorescence, together
484 with variously organized, penetrating biological structures. A high variability occurred in the
485 association of these phenomena with CUMBs, the microbial biofilm and different lichen
486 species, also depending on the considered blocks. However, CUMBs were mostly associated
487 with the absence of penetrating structures immediately beneath the rock surface, where a
488 white opalescent layer was a common trait. Such pattern was related with a higher presence of
489 calcite displaying the stabilization of the {01-12} calcite form, which is favoured by the
490 presence of organic substances (Pastero et al. 2003), in comparison with the fresh rock. Such
491 phenomenon was shared by several lichen-colonized samples, supporting the hypothesis of a
492 CUMBs-lichens relationship. In the following sub-sections, we discuss these findings,
493 summarized in Table S2, focusing on the elements of compatibility between CUMBs and
494 lichens and on features potentially informative on the CUMBs origin.

495 *4.1 Distributional and dimensional compatibility of CUMBs and lichens*

496 Investigations on lithobiontic colonization of natural marble surfaces, exposed following a
497 glacier retreat, showed rock-dwelling fungi, algae and cyanobacteria preceding the
498 colonization by lichens (Hoppert et al., 2004). Similarly, microbial biofilms are earlier

499 colonizers than lichens on carbonate heritage surfaces (Hoppert and König, 2006; Caneva et
500 al., 2008; Pinheiro et al. 2019). For algae and cyanobacterial, few years after a treatment can
501 be sufficient to a wide recolonization (Delgado Rodrigues et al, 2011; Bartoli et al, 2021). In
502 the case of the balustrade of Villa della Regina, considered about twenty years after the last
503 restoration, the darkening (av. $L^*=47.6$) due to the biofilm thoroughly affected its surface,
504 sparing CUMBs only, while lichen colonization was less widespread. Lichenometric studies,
505 aiming to date minimal surface exposure on the basis of lichen size, particularly focused on
506 longevity and mortality rates of the species more frequently used for this practical application.
507 In the case of *Rhizocarpon geographicum*, annual mortality rates between 0.4% and 5.1% of
508 thalli were reported for different sites, indicating a relatively low turnover of individuals in
509 natural populations (Osborn et al. 2015). Cleaning interventions by restorers radically change
510 this scenario, with a simultaneous removal of all thalli. With this regard, if lichens may leave
511 tracks of their colonization, these should be simultaneously appreciable on surfaces which
512 underwent restoration activity. The tracks should instead cyclically appear on natural surfaces,
513 likely resulting more sporadically, although these patterns would also generally depend on the
514 initial abundance of thalli. Accordingly, the high frequency of CUMBs on the marble
515 balustrade would suggest a high lichen colonization before the cleaning intervention at the
516 beginning of 2000s, but, unfortunately, the photographic documentation, although
517 highlighting the widespread biological colonization on the heritage surface, was not oriented
518 to detail the presence and distribution of the different lithobionts (Fig. S9). On the other hand,
519 with respect to the quarry surfaces, high heterogeneity of CUMBs frequency observed on the
520 blocks was significantly correlated with that of lichen thalli (Fig. S5). Such link between
521 lichen colonization and CUMBs may appear at odds with the detected dimensional
522 divergence, with thalli significantly larger than the uncolonized areas on the same surface.
523 However, on both the balustrade and the quarry blocks, CUMBs major axis appeared partially
524 superimposed to maxima values of lichen thalli (with the exception of block 3). With this
525 regard, it is worth noting that thalli measured on the balustrade are relatively young, as their
526 recolonization, even if immediately started after the cleaning, dates back approx. twenty
527 years, while thalli possibly occurring before the cleaning could be at a more mature growth
528 stage. Similarly, in the case of the quarry, maxima dimensions of the thalli may be expected to
529 correspond to their final stage of development, associated with decreased growth rates,
530 senescence, and, possibly, final detachment of the dead parts (Armstrong & Bradwell, 2010;
531 Osborn et al. 2015), and thus account for a further pattern of relationship with CUMBs. On
532 the rocks hosting many small thalli (*S. areolata* on blocks 1), CUMBs also display highest
533 density and minimal dimensions. Moreover, centimetric bare areas surrounding saxicolous
534 crustose lichens were reported in literature and related to the allelopathic potential of lichen
535 secondary metabolites, although few experiments have supported these field observations
536 (Armstrong and Welch, 2007). Similar clean surfaces were also observed on the balustrade,
537 around well-developed thalli of *Verrucaria* and *Circinaria* (Fig. S3). However, they were
538 more likely related to re-growths of the same species on surfaces they already occupied before
539 the cleaning, and from which they were not effectively removed, than to inhibitory halos.
540 Indeed, these phenomena were not thoroughly observed around all individuals, *V.*
541 *macrostoma* does not produce secondary lichen metabolites (Nimis 2022) and *C. gr. calcarea*
542 lacked asplicilin in the examined site. In the same context, the central parts of senescent thalli
543 were shown to degenerate, determining the formation of ‘windows’ available for new
544 colonization by the same or other species (Armstrong and Welch, 2007). The phenomenon
545 was also observed in the case of senescent thalli of *C. calcarea* (Pentecost, 1980). Similar

546 patterns may also justify colonization of black biofilms in the center of some larger CUMBs,
547 as those observed on the Caestia Pyramid (Caneva et al. 2020), on the balustrade and in the
548 case of block 6, although on the latter no lichen presence was observed.

549 *4.2 Microscopical and mineralogical features pointing to a CUMB - lichen relationships due*
550 *to stone physical modifications or allelopathic effects*

551 Colonization by biofilms and lichens also affects the marble interior, as observed on PAS-
552 stained sections from the quarry. The development of the hyphal penetration component
553 (*sensu* Favero-Longo et al. 2005) of lichens within marbles down to millimetric depths was
554 widely reported in literature (e.g., Hoppert et al. 2004; Garvie et al. 2008). In the examined
555 material, the values of massive and maximum penetration (*sensu* Favero-Longo et al. 2005,
556 2009) of *S. areolata*, down to 2.0 and 8.0 mm, respectively, were higher than the ranges of
557 0.3-0.7 mm and 1.0-3.0 mm, depending on the marble, reported for other epilithic species of
558 Verrucariaceae, as *Verrucaria nigrescens* and *V. macrostoma* (Favero-Longo et al. 2009).
559 Although the penetration of *Circinaria* gr. *calcareae* within the balustrade could not be
560 examined, it is worth noting that depths of massive and maximum penetration within marble
561 in the range 0.4-1.0 mm were reported for other species of the genus (*Circinaria contorta*;
562 Modenesi and Lajolo, 1988). A pattern of massive hyphal penetration down to 0.3 mm and
563 0.5 mm, respectively, combined with a strongly deeper network of thin hyphae down to
564 several millimeters, also characterized the endolithic *P. erodens* and *T. incavatum*. In
565 particular, the development of vertical channels by *P. erodens* was analogously observed for
566 the species within limestone (Pinna and Salvadori, 2000). The same ranges of penetration
567 were observed for *Thelidium absconditum* within Carrara marble (Workgroup ‘Cultural
568 Heritage’ of Lichen Italian Society, unpublished data). In all cases, penetration depths and
569 hyphal spread appeared lower than those observed for the same or phylogenetically related
570 species within limestone (Fry, 1922; Pinna et al. 1998; Matteucci et al., 2019; Tonon et al.
571 2022). Within the examined substrate, hyphal penetration was indeed limited to a sparse
572 intercrystalline penetration driven by the intrinsic textural properties, in particular the
573 medium-grained calcite, as already observed for species of genus *Verrucaria* colonizing other
574 poorly porous marbles (Favero-Longo et al., 2009). Similarly, the penetration of *C. contorta*
575 within marble was shown to exploit preexisting porosity between crystals, leaving an
576 impression on calcite crystals, but not penetrating them (Modenesi and Lajolo, 1988).

577 On the other hand, some hyphae and other PAS-stained biological structures were also
578 observed at deep layers, independent from lichen occurrences at the surface (i.e. also in
579 correspondence of CUMBs and biofilm), according to the high spread and diversity of
580 lithobionts growing endolithically characterized by molecular studies for marbles and other
581 lithologies (Bjelland and Ekman, 2005; Bjelland et al., 2011; Sajjad et al., 2022). The
582 characterization of such diversity of deep penetrating structures go beyond the interest of this
583 work and will be part of a subsequent paper. Nevertheless, the widespread biological
584 structures observed within the marble down to several millimeters of depth particularly
585 remarked the peculiarity of the absence of PAS-staining down to several hundreds of microns
586 beneath the CUMBs. In depth heavy growths contrasting low level of superficial colonization
587 were observed in volcanic rocks of an archaeological site, several decades after their
588 treatment with biocides, and evaluated as residues of previous colonizers (Caneva et al. 2005).
589 In the case of the marble quarry, the low colonization of CUMB surface rock layers (i.e. the
590 opalescent layer) at least in some blocks was followed by deep growths. Such observation
591 indicates for CUMBs a lower bioreceptivity not only at the marble surface, but also related to

592 the upper internal layers of the rock, suggesting some differences in intrinsic properties which
593 may favor or not the microbial colonization and penetration with respect to other areas.
594 Accordingly, Caneva and colleagues (2020) hypothesized that uncolonized circular areas on
595 the Caestia Pyramid may be related to a modification in the physical rock properties or to the
596 long-lasting presence of allelopathic substances. However, the production of secondary
597 metabolites was not a trait of the Verrucariaceae on the balustrade and the quarry blocks,
598 showing a dimensional compatibility with the CUMBs, and also *Circinaria* gr. *calcarea* at
599 Villa della Regina did not display the production of aspicilin considered by Caneva et al.
600 (2020) as a possible inhibitory agent on the Pyramid. On the other hand, the opalescent layer
601 displayed by CUMBs as a common trait, was also observed beneath lichens, while rarely
602 shared by the biofilm colonized surfaces (visualized in the PCoA by the positive relation of
603 the WL vector with CUMBs and most of lichens, opposed to biofilm marks). Similarly, color
604 shifts, associated or not to the loss of original textural features, were previously observed by
605 some of us in the upper layers of other carbonate rocks, namely the Portland and Botticino
606 limestones, when colonized by lichens, and putatively associated to their biogeochemical
607 activity (Morando et al., 2017). Other modifications of limestones colonized by lichens have
608 been also associated with an endolithic dissolution of calcite and the entrapment of organic
609 matter beneath the surface, determining some bioprotective effects (Concha-Lozano et al.,
610 2012). More in general, endolithic lichens were shown to determine a reprecipitation of fine-
611 grained calcite, building a protective coat on the colonized surfaces (Garvie et al., 2008). A
612 similar process was not microscopically observed for the examined marble, even by
613 cathodoluminescent investigations which could potentially discriminate calcites precipitated
614 in different conditions (Machel, 2000). However, XRPD analyses of calcite scraped from
615 CUMBs and lichens similarly showed some higher stabilization of the {01-12} form with
616 respect to biofilm colonized areas on the balustrade and fresh controls representative of quarry
617 blocks (with the exception of block 2). This behavior has been particularly associated to
618 calcite crystallization in presence of organic chelants (Pastero et al., 2003; Tonon et al., 2022),
619 providing some correlation of its higher frequency with biogeochemical processes.

620 Calcite dissolution and reprecipitation by lichens, including euendolithic ones (actively
621 dissolving calcite *sensu* Golubic et al. 1981), have been associated to different processes,
622 including a respiration-induced process only (Weber et al., 2011), but patterns are still not
623 generally understood (Pinna, 2021). Biogenic concretions after lichen thalli died were
624 associated to remains of oxalates (and carbonates) entrapping organic and mineral matter
625 (Ariño et al., 1995). In the case of the examined surfaces, oxalates were only detected in the
626 XRPD analyses performed beneath the *C. gr. Calcarea* on the balustrade. The release of the
627 common lichen-secreted chelant oxalic acid is not typically associated to the endolithic *P.*
628 *erodens* (Pinna and Salvadori, 2000) and the epilithic and endolithic Verrucariaceae (Pinna et
629 al., 1998), except for *Verrucaria rubrocincta* (Bungartz et al., 2004). However, aposymbiotic
630 cultures of some endolithic lichen species of Verrucariaceae demonstrated the production of
631 iron chelating molecules *in vitro* (Favero-Longo et al., 2011). On the other hand, both
632 calcicolous epilithic species of genus *Circinaria* and endolithic Verrucariaceae are known to
633 produce oil hyphae, which were the object of pioneer microscopic observations (Fry, 1922)
634 and subsequent chemical characterization of their lipid contents (Kushnir et al., 1978), but
635 their role has been not fully explained and was not connected with lichen biodeterioration
636 activities until now (Salvadori and Casanova Municchia, 2016; Jung and Budel, 2021).
637 However, as reported in the case of the alga *Acutodesmus obliquus* (Natsi et al., 2022), a high

638 concentration of lipids may increase the concentration of carboxylic groups within the
639 substrate, creating additional growth sites for calcite. With this regard, Modenesi and Lajolo
640 (1988) microscopically documented the capillary presence of oil droplets in the hyphae of *C.*
641 *contorta* penetrating within marble along its intercrystalline discontinuities. Although we did
642 not investigate the presence of oil hyphae, this mentioned literature provides some support to
643 the hypothesis that the hyphal penetration component of lichens can provide the organic
644 compounds responsible for the stabilization of the calcite {01-12} form during a
645 reprecipitation process. How the cleaning operations, by removing the thalli and their
646 photobiont later, may promote such hypothesized process and, thus, further relate with
647 CUMBs is worth of future investigations.

648 Biological reprecipitation processes were related to bioprotective effects, due to the
649 development of surface coatings and the closure of discontinuities between mineral grains,
650 reducing substrate porosity (Gadd and Dyer, 2017). Despite the hyphal penetration, lichen
651 cover can determine an unmodified or even reduced water absorption by different lithic
652 substrates, until the thalli are not mechanically removed from the surfaces, reverting the
653 pattern (Morando et al., 2017; Pinna et al., 2023). The performed absorption tests agreed with
654 this latter scenario, with CUMBs absorbing more water than the nearby colonized surfaces
655 (considered after the biofilm removal). This observation supports the hypothesis that a
656 previous lichen penetration could have increased the substrate porosity by their physical
657 action (Modenesi and Lajolo, 1988; Garvie et al., 2008; Favero-Longo et al., 2009), while
658 leaves unresolved the reasons of the lower bioreceptivity, which contrasts with the higher
659 water availability within the substrate (Sanmartín et al., 2021).

660 The presence of organic matter within carbonate rocks was associated to the observation of
661 fluorescence phenomena (Tyson, 2012). These were limited to the upper rock layers, thus
662 ruling out a correlation with general impurities of the examined marble, and rather addressing
663 a surface-localized concentration related to the presence of lithobionts. If Verrucariaceae are
664 not producers of lichen secondary metabolites, often associated to autofluorescence under UV
665 light (Orange et al., 2001), *C. pusilla* and *P. erodens* are known to produce antraquinones,
666 which can have allelopathic functions (Gazzano et al., 2013), and the related alternative
667 pigment “*sedifolia* grey”, respectively (Nimis, 2022). However, fluorescence phenomena
668 were also variously associated to the microbial biofilm on block 6, *S. areolata* on block 1, and
669 other CUMBs, preventing a direct correlation with a certain lithobiontic component and the
670 CUMBs (visualized in the PCoA by the superimposed orientation of all the fluorescence
671 vectors in the third quadrant). Other approaches are thus necessary to target the potential
672 presence of allelopathic substances entrapped in the reprecipitated calcite, according to the
673 hypothesis by Caneva and colleagues (2020). With this regard, Raman spectroscopy already
674 allowed the detection of secondary metabolites as biomarkers of past colonization of rocks by
675 lichens (Casanova-Municchia et al., 2014), and thus appears a promising approach for future
676 steps of this research. Nevertheless, it is also worth noting that successive generations of
677 different lithobionts may potentially superimpose their effects and metabolite traces,
678 justifying the complex detected scenario (Morando et al., 2017).

679 In the analyzed case, a CUMBs-lichens relationship is thus suggested by some microscopical
680 and mineralogical features (first of all calcite reprecipitation and the whitish opalescent layer
681 beneath both lichens and CUMBs), together with field evidence of frequent co-presence and a
682 morphometric and distributional compatibility. It is worth remembering that the CUMBs
683 phenomenon was here examined on surfaces in different climatic zones (Köppen-Geiger Cfa

684 and Dfc zones), but sharing, as common conditions, an exposure to direct sun irradiation and
685 the marble lithology. Further investigations are necessary to extend the comprehension of
686 ecological conditions associated to the lichen-origin of such CUMBs phenomenon and the
687 differences with those connected with other causative factors (see Fig. 1).

688

689 **5 Conclusion**

690 This work characterized centimetric circular areas left free from biofilm (re-)colonization on
691 marble surfaces of both cultural heritage and quarry sites, showing elements of morphometric,
692 distributional, microscopical and mineralogical compatibility with tracks of a past lichen
693 colonization. In particular, CUMBs and lichen colonized surfaces shared evidences of calcite
694 reprecipitation, that may affect physical properties of the upper internal layers of the rock and,
695 thus, their bioreceptivity. However, observations also indicated a surface-localized
696 concentration of organic matter, which is worth of further spectroscopic investigations to
697 evaluate the potential occurrence of allelopathic compounds. Clarifying an effective
698 combination of physical modification and enrichment in bioactive molecules of the surface
699 marble layers may drive the implementation of innovative strategies to prevent recolonization
700 of stone cultural heritage.

701

702 **6 Acknowledgements**

703 This study was funded by University of Torino grants (RiLo). The authors are grateful to
704 Alessandra Guerrini, Laura Moro, and Chiara Teolato (Direzione Regionale Musei Piemonte,
705 previously Polo Museale del Piemonte) for permission to access the Villa della Regina for this
706 study, and to all the personnel of the monumental site for logistic support. Moreover, the
707 authors thanks Enrica Matteucci, Mariagrazia Morando, Greta Rao Torres, Alessia Romano,
708 Silvia Sciacca, Chiara Tonon (University of Torino) and Paola Iacomussi (INRIM) for
709 assistance during some phases of fieldwork and helpful discussions, and two anonymous
710 reviewers for their valuable suggestions to improve the clarity of the manuscript.

711

712 **7. References**

- 713 Ariño, X., Ortega-Calvo, J. J., Gomez-Bolea, A., Saiz-Jimenez, C., 1995. Lichen colonization
714 of the Roman pavement at Baelo Claudia (Cadiz, Spain): biodeterioration vs. bioprotection.
715 *Science of the Total Environment* 167, 353-363. doi.org/10.1016/0048-9697(95)04595-R
- 716 Armstrong, R. A., Welch, A. R., 2007. Competition in lichen communities. *Symbiosis* 43, 1-
717 12.
- 718 Armstrong, R., Bradwell, T., 2010. Growth of crustose lichens: a review. *Geografiska*
719 *Annaler: Series A, Physical Geography*, 92, 3-17. doi.org/10.1111/j.1468-0459.2010.00374.x
- 720 Bartoli, F., Casanova Municchia, A., Futagami, Y., Kashiwadani, H., Moon, K.H., Caneva,
721 G., 2014. Biological colonization patterns on the ruins of Angkor temples (Cambodia) in the
722 biodeterioration vs bioprotection debate. *International Biodeterioration and Biodegradation*
723 96, 157-165. doi.org/10.1016/j.ibiod.2014.09.015
- 724 Bartoli, F., Casanova Municchia, A., Leotta, M., Luciano, S. and Caneva, G., 2021.
725 Biological recolonization dynamics: Kentridge's artwork disappearing along the Tiber

- 726 embankments (Rome, Italy). *International Biodeterioration & Biodegradation* 160, 105214.
727 doi.org/10.1016/j.ibiod.2021.105214
- 728 Bjelland, T., Ekman, S., 2005. Fungal diversity in rock beneath a crustose lichen as revealed
729 by molecular markers. *Microbial ecology* 49, 598-603. doi.org/10.1007/s00248-004-0101-z
- 730 Bjelland, T., Grube, M., Hoem, S., Jorgensen, S. L., Daae, F. L., Thorseth, I. H., Øvreås, L.,
731 2011. Microbial metacommunities in the lichen–rock habitat. *Environmental Microbiology*
732 *Reports* 3, 434-442. doi.org/10.1111/j.1758-2229.2010.00206.x
- 733 Borghi, A., d’Atri, A., Martire, L., Castelli, D., Costa, E., Dino, G., Favero Longo, S. E.,
734 Ferrando, L., Gallo, M., Giardino, M., Groppo, C., Piervittori, R., Rolfo, F., Rossetti, P.,
735 Vaggelli, G., 2014. Fragments of the Western Alpine chain as historic ornamental stones in
736 Turin (Italy): enhancement of urban geological heritage through geotourism. *Geoheritage* 6,
737 41-55. doi.org/10.1007/s12371-013-0091-7
- 738 Bungartz, F., Garvie, L. A., 2004. Anatomy of the endolithic Sonoran Desert lichen
739 *Verrucaria rubrocincta* Breuss: implications for biodeterioration and biomineralization. *The*
740 *Lichenologist* 36, 55-73. doi.org/10.1017/S0024282904013854
- 741 Caneva, G., Salvadori, O., Ricci, S., & Ceschin, S., 2005. Ecological analysis and
742 biodeterioration processes over time at the Hieroglyphic Stairway in the Copán (Honduras)
743 archaeological site. *Plant Biosystems* 139, 295-310. doi.org/10.1080/11263500500343353
- 744 Caneva, G., Nugari, M. P., Salvadori, O., (Eds.), 2008. *Plant biology for cultural heritage:*
745 *biodeterioration and conservation.* Getty Publications.
- 746 Caneva, G., Lombardozzi, V., Ceschin, S., Casanova Municchia, A., and Salvadori, O., 2014.
747 Unusual differential erosion related to the presence of endolithic microorganisms (Martvili,
748 Georgia). *Journal of Cultural Heritage* 15, pp.538-545. doi.org/10.1016/j.culher.2013.10.003
- 749 Caneva, G., Fidanza, M. R., Tonon, C., Favero-Longo, S. E., 2020. Biodeterioration patterns
750 and their interpretation for potential applications to stone conservation: A hypothesis from
751 allelopathic inhibitory effects of lichens on the Caestia Pyramid (Rome). *Sustainability* 12,
752 1132. doi.org/10.3390/su12031132
- 753 Carter, N. E. A., Viles, H. A., 2005. Bioprotection explored: the story of a little-known earth
754 surface process. *Geomorphology* 67, 273-281. doi.org/10.1016/j.geomorph.2004.10.004
- 755 Chen, J., Blume, H. P., Beyer, L., 2000. Weathering of rocks induced by lichen
756 colonization—a review. *Catena* 39, 121-146. doi.org/10.1016/S0341-8162(99)00085-5
- 757 Concha-Lozano, N., Gaudon, P., Pages, J., De Billerbeck, G., Lafon, D., Eterradosi, O.,
758 2012. Protective effect of endolithic fungal hyphae on oolitic limestone buildings. *Journal of*
759 *Cultural Heritage* 13, 120-127. doi.org/10.1016/j.culher.2011.07.006
- 760 Cuberos – Cáceres, L., Calvo-Bayo, I., Romero-Noguera, J., Bolivar-Galiano, F., 2022. Study
761 and development of a new methods to inhibit the growth of biofilm in the ornamental
762 fountains of the Alhambra and the Generalife, In: Di Martino, P., Cappitelli, F., Villa, F.,
763 Bruno, L., (Eds.), *ECBSM 2022-European Conference on Biodeterioration of Stone*
764 *Monuments* (5th ed.), pp. 36.
- 765 Danin, A. Caneva, G., 1990. Deterioration of limestone walls in Jerusalem and marble
766 monuments in Rome caused by cyanobacteria and cyanophilous lichens. *International*
767 *biodeterioration* 26, 397-417. doi.org/10.1016/0265-3036(90)90004-Q

768 Delgado Rodrigues, J., Anjos, M.V., Charola, A.E., 2011. Recolonization of marble
769 sculptures in a garden environment, in: Charola, A.E., McNamara, C., Koestler, R. (Eds.),
770 Biocolonization of stone: Control and preventive methods. Smithsonian contributions to
771 museum conservation, 2. Smithsonian Institution Scholarly Press, Washington, pp. 71-85.

772 de los Ríos, A., Souza-Egipsy, V., 2021. The interface of rocks and microorganisms. In:
773 Burkhard Büdel, B., Friedl, T., (Eds.), Life at Rock Surfaces, De Gruyter, Berlin, pp. 3-38.
774 doi.org/10.1515/9783110646467

775 Dyer, T., 2017. Deterioration of stone and concrete exposed to bird excreta examination of the
776 role of glyoxylic acid. International Biodeterioration and Biodegradation 125, 125-141.
777 doi.org/10.1016/j.ibiod.2017.09.002

778 Edwards, H. G., Seaward, M. R., Attwood, S. J., Little, S. J., de Oliveira, L. F., & Tretiach,
779 M., (2003). FT-Raman spectroscopy of lichens on dolomitic rocks: an assessment of metal
780 oxalate formation. Analyst, 128(10), 1218-1221. doi.org/ 10.1039/B306991P

781 EN 17655, 2021. Conservation of cultural heritage - Determination of water absorption by
782 contact sponge method.

783 Favero-Longo, S. E., Castelli, D., Salvadori, O., Belluso, E., Piervittori, R., 2005. Pedogenetic
784 action of the lichens *Lecidea atrobrunnea*, *Rhizocarpon geographicum* gr. and *Sporastatia*
785 *testudinea* on serpentinized ultramafic rocks in an alpine environment. International
786 Biodeterioration and Biodegradation 56, 17-27. doi.org/10.1016/j.ibiod.2004.11.006

787 Favero-Longo, S. E., Borghi, A., Tretiach, M., Piervittori, R., 2009. In vitro receptivity of
788 carbonate rocks to endolithic lichen-forming aposymbionts. Mycological research 113, 1216-
789 1227. doi.org/10.1016/j.mycres.2009.08.006

790 Favero-Longo, S. E., Gazzano, C., Girlanda, M., Castelli, D., Tretiach, M., Baiocchi, C.,
791 Piervittori, R., 2011. Physical and chemical deterioration of silicate and carbonate rocks by
792 meristematic microcolonial fungi and endolithic lichens (Chaetothyriomycetidae).
793 Geomicrobiology Journal 28, 732-744. doi.org/10.1080/01490451.2010.517696

794 Favero-Longo, S.E., Viles, H.A, 2020. A Review of the Nature, Role and Control of
795 Lithobionts on Stone Cultural Heritage: Weighing-up and Managing Biodeterioration and
796 Bioprotection. World Journal of Microbiology and Biotechnology 36, 7.
797 doi.org/10.1007/s11274-020-02878-3

798 Fry, E. J., 1922. Some types of endolithic limestone lichens. Annals of Botany 36, 541-562.

799 Gadd, G. M., 2017. Geomicrobiology of the built environment. Nature microbiology 2, 1-9.
800 doi.org/10.1038/nmicrobiol.2016.275

801 Gadd, G. M., Dyer, T. D., 2017. Bioprotection of the built environment and cultural heritage.
802 Microbial Biotechnology 10, 1152-1156. doi.org/10.1111/1751-7915.12750

803 Garvie, L. A., Knauth, L. P., Bungartz, F., Klonowski, S., Nash, T. H., 2008. Life in extreme
804 environments: survival strategy of the endolithic desert lichen *Verrucaria rubrocincta*.
805 Naturwissenschaften 95, 705-712. doi.org/10.1007/s00114-008-0373-0

806 Gazzano, C., Favero-Longo, S. E., Matteucci, E., Piervittori, R., 2009. Image analysis for
807 measuring lichen colonization on and within stonework. The Lichenologist 41, 299-313.
808 doi.org/10.1017/S0024282909008366

- 809 Gazzano, C., Favero-Longo, S. E., Iacomussi, P., Piervittori, R., 2013. Biocidal effect of
810 lichen secondary metabolites against rock-dwelling microcolonial fungi, cyanobacteria and
811 green algae. *International Biodeterioration and Biodegradation* 84, 300-306.
812 doi.org/10.1016/j.ibiod.2012.05.033
- 813 Ghelli, A., 2004. Marmi di Rocca Bianca. Tra particolarità litologiche e sapiente sfruttamento
814 antropico. In: Aigotti, D., (Eds.), *I geositi nel paesaggio alpino della Provincia di Torino*, Vol.
815 1, Litografia Geda di Nichelino, Torino, pp. 75-80.
- 816 Golubic, S., Friedmann, E. I., Schneider, J., 1981. The lithobiontic ecological niche, with
817 special reference to microorganisms. *Journal of Sedimentary Research* 51, 475-478.
818 doi.org/10.1306/212F7CB6-2B24-11D7-8648000102C1865D
- 819 Guglielmin, M., Favero-Longo, S. E., Cannone, N., Piervittori, R., Strini, A., 2011. Role of
820 lichens in granite weathering in cold and arid environments of continental Antarctica.
821 *Geological Society Special Publications* 354, 195-204. doi.org/10.1144/SP354.12
- 822 Guillitte, O., 1995. Bioreceptivity: a new concept for building ecology studies. *Science of the*
823 *total environment* 167, 215-220. doi.org/10.1016/0048-9697(95)04582-L
- 824 Hoppert, M., Flies, C., Pohl, W., Günzl, B., Schneider, J., 2004. Colonization strategies of
825 lithobiontic microorganisms on carbonate rocks. *Environmental Geology* 46, 421-428.
826 doi.org/10.1007/s00254-004-1043-y
- 827 Hoppert, M., König, S., 2006. The succession of biofilms on building stone and its possible
828 impact on biogenic weathering. *Heritage, weathering and conservation* 2, 311-315.
- 829 ISO/CIE 11664-4, 2019. Colorimetry — Part 4: CIE 1976 L*a*b* colour space.
- 830 Jung, P., Büdel, B., 2021. Lichens as pioneers on rock surfaces. In: Burkhard Büdel, B.,
831 Friedl, T., (Eds.), *Life at Rock Surfaces*, De Gruyter, Berlin, pp. 141-160.
832 doi.org/10.1515/9783110646467
- 833 Kottke, M., Grieser, J., Beck, C., Rudolf, B., Rubel, F., 2006. World map of the Köppen-
834 Geiger climate classification updated. *Meteorologische Zeitschrift* 15, 259-263.
835 doi.org/10.1127/0941-2948/2006/0130
- 836 Kushnir, E., Tietz, A., Galun, M., 1978. "Oil hyphae" of endolithic lichens and their fatty acid
837 composition. *Protoplasma* 97, 47-60. doi.org/10.1007/BF01276389
- 838 Lombardozi, V., Castrignanò, T., D'Antonio, M., Casanova Municchia, A., Caneva, G.,
839 2012. An interactive database for an ecological analysis of stone biopitting. *International*
840 *Biodeterioration and Biodegradation* 73, 8-15. doi.org/10.1016/j.ibiod.2012.04.016
- 841 Machel, H.G., 2000. Application of cathodoluminescence to carbonate diagenesis. In: Pagel,
842 M., Barbin, V., Blanc, P., Ohnenstetter, D., (Eds.), *Catodoluminescence in Geosciences*,
843 Springer, Berlin, Heidelberg, pp. 271- 302. doi.org/10.1007/978-3-662-04086-7_11
- 844 Marini, P., Mossetti C., 2006. Natural stones used in a Royal House of Piedmont (Italy). In:
845 Fort, R., Alvarez de Buergo, M., Gomez-Heras, M., Vazquez-Calvo, M., (Eds.), *Proceedings*
846 *of the International Conference on Heritage, Weathering and Conservation*, Vol. 2, Taylor &
847 Francis Group, London, pp. 895-900.
- 848 Matteucci, E., Scarcella, A. V., Croveri, P., Marengo, A., Borghi, A., Benelli, C., Hamdan,
849 O., Favero-Longo, S. E., 2019. Lichens and other lithobionts on the carbonate rock surfaces of

850 the heritage site of the tomb of Lazarus (Palestinian territories): diversity, biodeterioration,
851 and control issues in a semi-arid environment. *Annals of Microbiology* 69, 1033-1046.
852 doi.org/10.1007/s13213-019-01465-8

853 McIlroy de la Rosa, J. P., Warke, P. A., Smith, B. J., 2013. Lichen-induced biomodification of
854 calcareous surfaces: bioprotection versus biodeterioration. *Progress in Physical Geography*
855 37, 325-351. doi.org/10.1177/0309133312467660

856 McIlroy de la Rosa, J. P., Warke, P. A., Smith, B. J., 2014. The effects of lichen cover upon
857 the rate of solutional weathering of limestone. *Geomorphology* 220, 81-92.
858 doi.org/10.1016/j.geomorph.2014.05.030

859 Miralles, I., Edwards, H.G., Domingo, F., Jorge-Villar, S.E., 2015. Lichens around the world:
860 a comprehensive study of lichen survival biostrategies detected by Raman spectroscopy.
861 *Analytical Methods* 7, 6856-6868. doi.org/ 10.1039/C5AY00655D

862 Modenesi, P., Lajolo, L., 1988. Microscopical investigation on a marble encrusting lichen.
863 *Studia Geobotanica* 8, pp. 47-64.

864 Morando, M., Wilhelm, K., Matteucci, E., Martire, L., Piervittori, R., Viles, H. A.,
865 Favero- Longo, S. E., 2017. The influence of structural organization of epilithic and
866 endolithic lichens on limestone weathering. *Earth Surface Processes and Landforms* 42, 1666-
867 1679. doi.org/10.1002/esp.4118

868 Natsi, P. D., Koutsoukos, P. G., 2022. Calcium Carbonate Mineralization of Microalgae.
869 *Biomimetics* 7, 140. doi.org/10.3390/biomimetics7040140

870 Nimis, P.L., 2022. ITALIC - The Information System on Italian Lichens. Version 7.0.
871 University of Trieste, Dept. of Biology. <https://dryades.units.it/italic>, accessed on 2022, 12.

872 Nimis, P.L., Martellos, S., 2020. Towards a digital key to the lichens of Italy. *Symbiosis* 82,
873 149-155. doi.org/10.1007/s13199-020-00714-8

874 Nimis, P.L., Pinna, D., Salvadori, O., 1992. *Licheni e conservazione dei monumenti*. CLU
875 Editrice, Bologna, Italy.

876 Orange, A., James, P. W., White, F. J., 2001. Microchemical methods for the identification of
877 lichens. *British Lichen Society*.

878 Osborn, G., McCarthy, D., LaBrie, A., Burke, R., 2015. Lichenometric dating: science or
879 pseudo-science?. *Quaternary Research* 83, 1-12. doi.org/10.1016/j.yqres.2014.09.006

880 Pastero, L., Costa, E., Alessandria, B., Rubbo, M., Aquilano, D., 2003. The competition
881 between {1014} cleavage and {0112} steep rhombohedra in gel grown calcite crystals.
882 *Journal of crystal growth* 247, 472-482. doi.org/10.1016/S0022-0248(02)01911-5

883 Pentecost, A., 1980. Aspects of competition in saxicolous lichen communities. *The*
884 *Lichenologist* 12, 135-144. doi.org/10.1017/S0024282980000060

885 Piervittori, R., Salvadori, O., Seaward, M.R.D., 2004. Lichens and monuments. In: St.Clair,
886 L.L., Seaward, M.R.D., (Eds.), *Biodeterioration of stone surfaces. Lichens and biofilms as*
887 *weathering agents of rocks and Cultural Heritage*. Kluwer Academic Publishers, Dordrecht,
888 pp. 241-282. doi.org/ 10.1007/978-1-4020-2845-8_2

889 Pinheiro, A. C., Mesquita, N., Trovão, J., Soares, F., Tiago, I., Coelho, C., de Carvalho, H.P.,
890 Gil, F., Catarino, L., Piñar, G., Portugal, A., 2019. Limestone biodeterioration: A review on

891 the Portuguese cultural heritage scenario. *Journal of cultural heritage* 36, 275-285.
892 doi.org/10.1016/j.culher.2018.07.008

893 Pinna, D., Salvadori, O., Tretiach, M., 1998. An anatomical investigation of calcicolous
894 endolithic lichens from the Trieste karst (NE Italy). *Plant Biosystems* 132, 183-195.
895 doi.org/10.1080/11263504.1998.10654203

896 Pinna, D., Salvadori, O., 2000. Endolithic lichens and conservation: an underestimated
897 question. In: Fassina, V., (Ed.), *Proceedings of the 9th International Conference on*
898 *Deterioration and Conservation of Stone*, Vol. 1. Elsevier, Amsterdam, pp. 513-519.
899 doi.org/10.1016/B978-044450517-0/50136-7

900 Pinna, D., 2021. Microbial growth and its effects on inorganic heritage materials. In: Joseph,
901 E., (Ed.), *Microorganisms in the Deterioration and Preservation of Cultural Heritage*. Springer
902 Nature, pp. 3-35. doi.org/10.1007/978-3-030-69411-1

903 Pinna, D., Mazzotti, V., Gualtieri, S., Voyron, S., Andreotti, A., Favero-Longo, S. E., 2023.
904 Damaging and protective interactions of lichens and biofilms on ceramic dolia and sculptures
905 of the International Museum of Ceramics, Faenza, Italy. *Science of The Total Environment*
906 877, 162607. doi.org/10.1016/j.scitotenv.2023.162607

907 Sajjad, W., Ilahi, N., Kang, S., Bahadur, A., Zada, S., Iqbal, A., 2022. Endolithic microbes of
908 rocks, their community, function and survival strategies. *International Biodeterioration and*
909 *Biodegradation* 169, 105387. doi.org/10.1016/j.ibiod.2022.105387

910 Salvadori, O., Casanova Municchia, A., 2016. The role of fungi and lichens in the
911 biodeterioration of stone monuments. *The Open Conference Proceedings Journal* 7, 39–54.
912 doi.org/10.2174/2210289201607020039

913 Sanmartín, P., Miller, A. Z., Prieto, B., Viles, H. A., 2021. Revisiting and reanalysing the
914 concept of bioreceptivity 25 years on. *Science of The Total Environment* 770, 145314.
915 doi.org/10.1016/j.scitotenv.2021.145314

916 Seaward, M. R., 2015. Lichens as agents of biodeterioration. *Recent Advances in*
917 *Lichenology: Modern Methods and Approaches in Biomonitoring and Bioprospection* 1, 189-
918 211. doi.org/10.1007/978-81-322-2181-4_9

919 Slavík, M., Bruthans, J., Filippi, M., Schweigstillová, J., Falteisek, L., Řihošek, J., 2017.
920 Biologically-initiated rock crust on sandstone: Mechanical and hydraulic properties and
921 resistance to erosion. *Geomorphology* 278, 298-313. doi.org/10.1016/j.geomorph.2016.09.040

922 Ter Braak, C.J.F., Šmilauer, P., 2002. *CANOCO reference manual and CanoDraw for*
923 *Windows user's guide: software for canonical community ordination (version 4.5)*. Ithaca,
924 NY: Microcomputer Power, pp. 500.

925 Tonon, C., Bernasconi, D., Martire, L., Pastero, L., Viles, H., Favero- Longo, S. E., 2022.
926 Lichen impact on sandstone hardness is species- specific. *Earth Surface Processes and*
927 *Landforms* 47, 1147-1156. doi.org/10.1002/esp.5307

928 Tyson, R. V., 2012. *Sedimentary organic matter: organic facies and palynofacies*. Springer
929 Science & Business Media.

930 Vergès-Belmin, V., 2008. *Illustrated glossary on stone deterioration patterns*. Icomos.

- 931 Weber, B., Scherr, C., Bicker, F., Friedl, T., Büdel, B., 2011. Respiration- induced
932 weathering patterns of two endolithically growing lichens. *Geobiology* 9, 34-43.
933 doi.org/10.1111/j.1472-4669.2010.00256.x
- 934 Whitlatch, R. B., Johnson, R. G., 1974. Methods for staining organic matter in marine
935 sediments. *Journal of Sedimentary Research* 44, 1310-1312. doi.org/10.1306/212F6CAD-
936 2B24-11D7-8648000102C1865D
- 937

939 **Captions:**

940 **Fig. 1.** The phenomenon of CUMBs observed on different stone surfaces. (A) Marble statue
 941 in the Monumental Cemetery of Milan (Italy); (B) marble statue in Parma (Italy); (C) cement
 942 pavement, beneath a fig tree, in Saint Jean Cap-Ferrat near Nice (France); (D) cement
 943 balustrade in the Kasteel de Haar near Utrecht (Netherlands); (E) marble balustrade and (F)
 944 marble statue in the Monumental Cemetery of Milan (Italy); (G-H) sandstone pavements of
 945 the walls of Aigues-Mortes (France; G) and of the Palace of the Popes in Avignon (France;
 946 H). Arrows indicate CUMBs; # indicate lichens in the nearby (in the inset in H).

947 **Fig. 2.** CUMB patterns on marble surfaces at the Villa della Regina (A-C) and the quarry of
 948 Rocca Bianca (D-F). (A) Widespread dark microbial biofilm on a balustrade capstone,
 949 interrupted by the presence of CUMBs; (B) CUMBs (*) and a lichen thallus of *Circinaria* gr.
 950 *calcareae* of similar dimensions (#); (C) uncolonized areas adjacent to thalli of *Verrucaria*
 951 *macrostoma* in the direction of the water washout from the capstone (*); (D) slightly inclined
 952 surfaces of blocks 1a-d with CUMBs and co-occurring brown epilithic thalli of *Staurothele*
 953 *areolata*; (B) block 2, vertical surface with larger CUMBs interposed to a continuous
 954 pluricentimetric colonization of the same *S. areolata*; (C) block 3 horizontal surface with
 955 CUMBs, small thalli of *S. areolata* (#) surrounded by uncolonized circular borders, and thalli
 956 of the endolithic species *Thelidium incavatum* (*); (D) mosaic of CUMBs on the horizontal
 957 surface of block 4, mostly colonized by epilithic thalli of *Caloplaca pusilla* (+) and endolithic
 958 thalli of *T. incavatum* (*) and, subordinately, *Pyrenodesmia erodens* (§); (E) block 5
 959 horizontal surface with CUMBs, co-occurring thalli of *P. erodens* and a dark microbial
 960 biofilm; (F) block 6 vertical surface with CUMBs displaying their center colonized by a dark
 961 biofilm.

962 **Fig. 3.** Morphometric analysis (length of main axis, A-B, and circularity, C-D) of CUMBs
 963 and lichens on (A, C) the balustrade at the Villa della Regina (Verr, *Verrucaria macrostoma*;
 964 Circ, *Circinaria* gr. *calcareae*; Xant, *Xanthocarpia crenulatella*; Cand, *Candelariella aurella*;
 965 Myr, *Myriolecis dispersa*) and (B, D) at the quarry of Rocca Bianca, separately considered for
 966 blocks 1-6 (blocks 1-3, Sta, *Staurothele areolata*; 4-5, Pyr, *Pyrenodesmia erodens*). Boxplots
 967 show 95th percentile (upper whisker), 75th percentile (top box), median (transversal line),
 968 mean (small square), 25th percentile (bottom box), 5th percentile (lower whisker). With
 969 reference to the balustrade and per each block of the quarry, box-plots not sharing at least one
 970 letter are significantly different (ANOVA with Tukey's post-hoc test, $p < 0.05$).

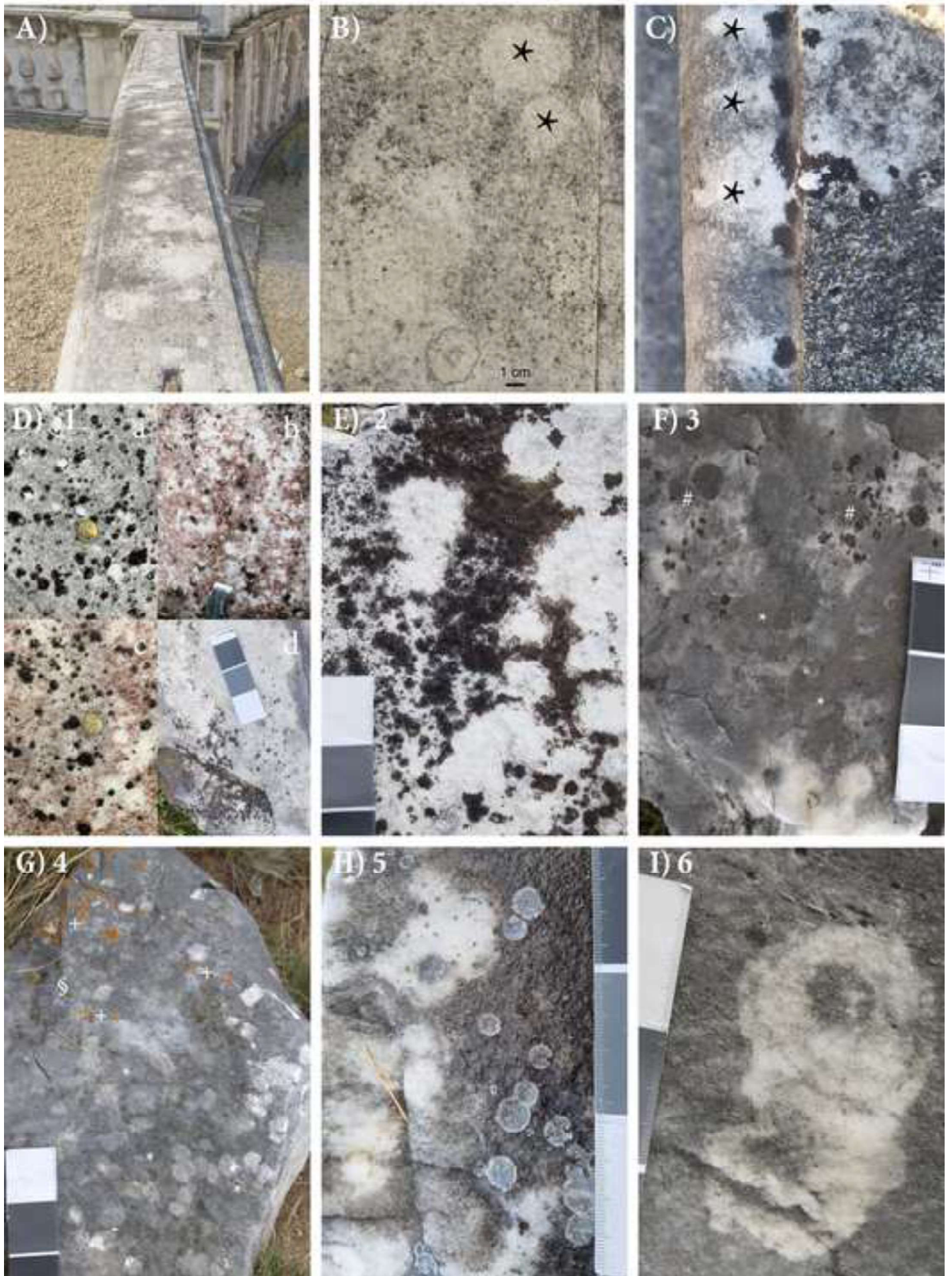
971 **Fig. 4.** Lightness (L^*) and a^*/b^* ratios of CUMBs (blue dots) and their biofilm colonized
 972 surrounding areas (orange dots) on (A) the balustrade of Villa della Regina and on (B) the
 973 marble blocks of the quarry of Rocca Bianca. For the quarry blocks, measures obtained from
 974 freshly cut surfaces are also reported (grey dots).

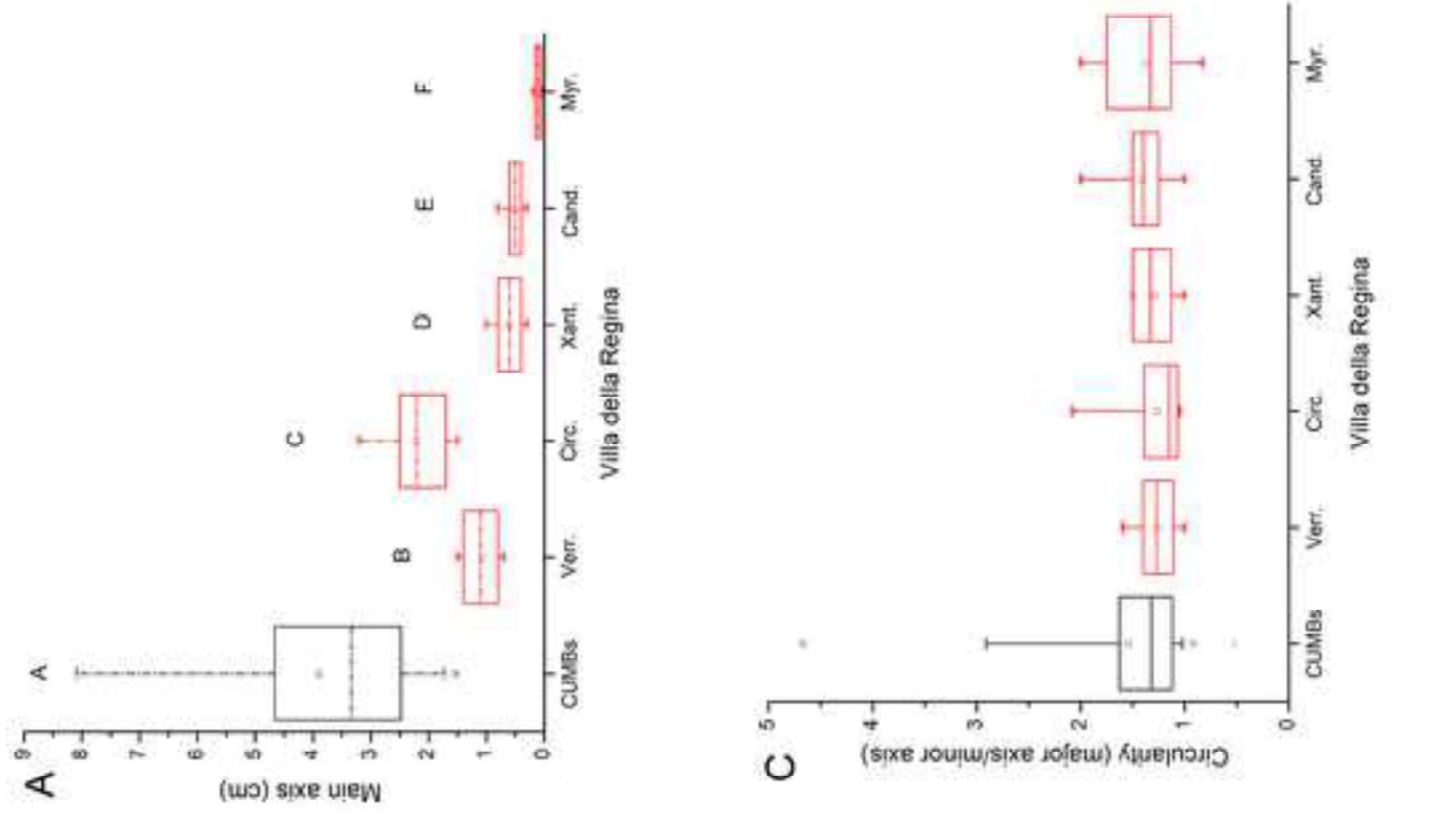
975 **Fig. 5.** Water absorption in correspondence of the CUMBs and the surrounding colonized
 976 areas, expressed as ratio between the two values (black boxplots). In the case of the quarry,
 977 the measures were repeated after the cleaning of the biofilm (red boxplot). Values shown by
 978 box-plots as in Fig. 3; box-plots not sharing at least one letter are significantly different
 979 (ANOVA with Tukey's post-hoc test, $p < 0.05$).

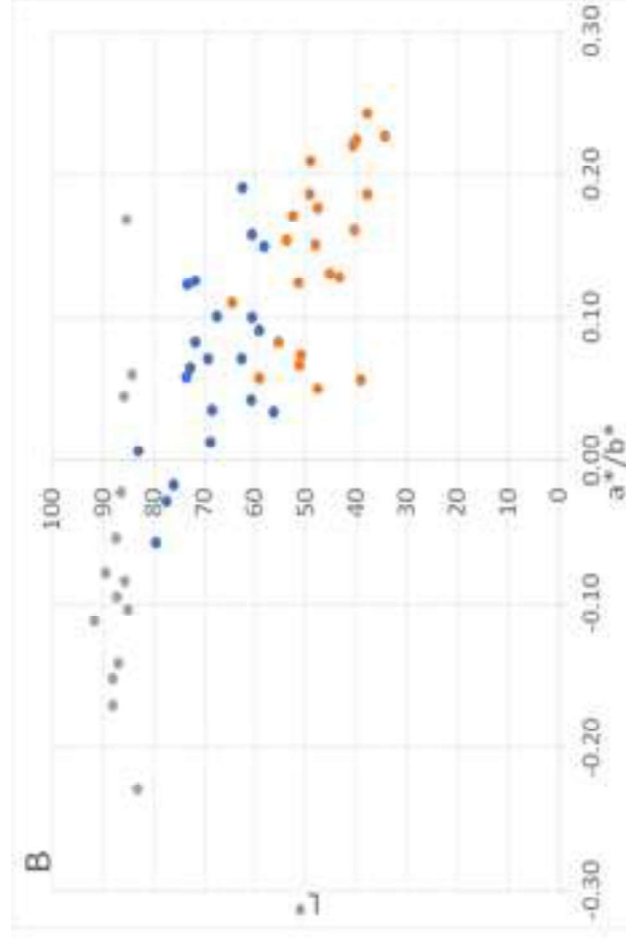
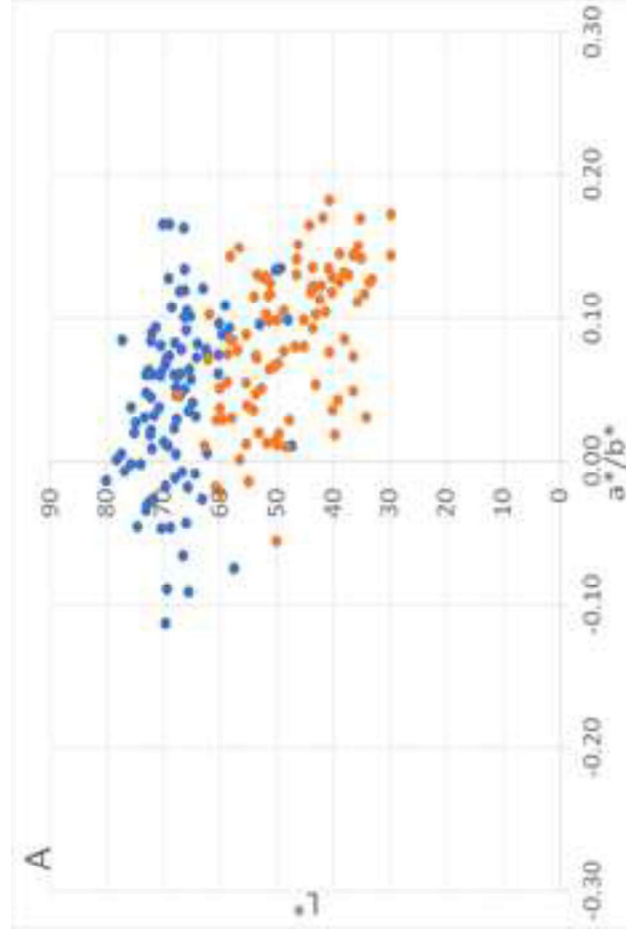
980 **Fig. 6.** XRPD analyses. (A) percentage difference between the $(I/WHM)_{\text{Cal } 01-12}/(I/WHM)_{\text{Cal } 10-14}$ ratios calculated for the CUMBs and the lichens (*Circ*, *Circinaria*
981 *calcareo*; *Verr*, *Verrucaria macrostoma*) with respect to the nearby areas colonized by
982 biofilms; (B) percentage difference between the $(I/WHM)_{\text{Cal } 01-12}/(I/WHM)_{\text{Cal } 10-14}$ ratios
983 calculated for the CUMBs and the different blocks (6. biofilm; 1. *Staurothele areolata*; 5
984 *Thelidium incavatum* and *Pyrenodesmia erodens*; 2. *Staurothele areolata*) with respect to the
985 fresh unexposed stone. Values shown by box-plots as in Fig. 3.
986

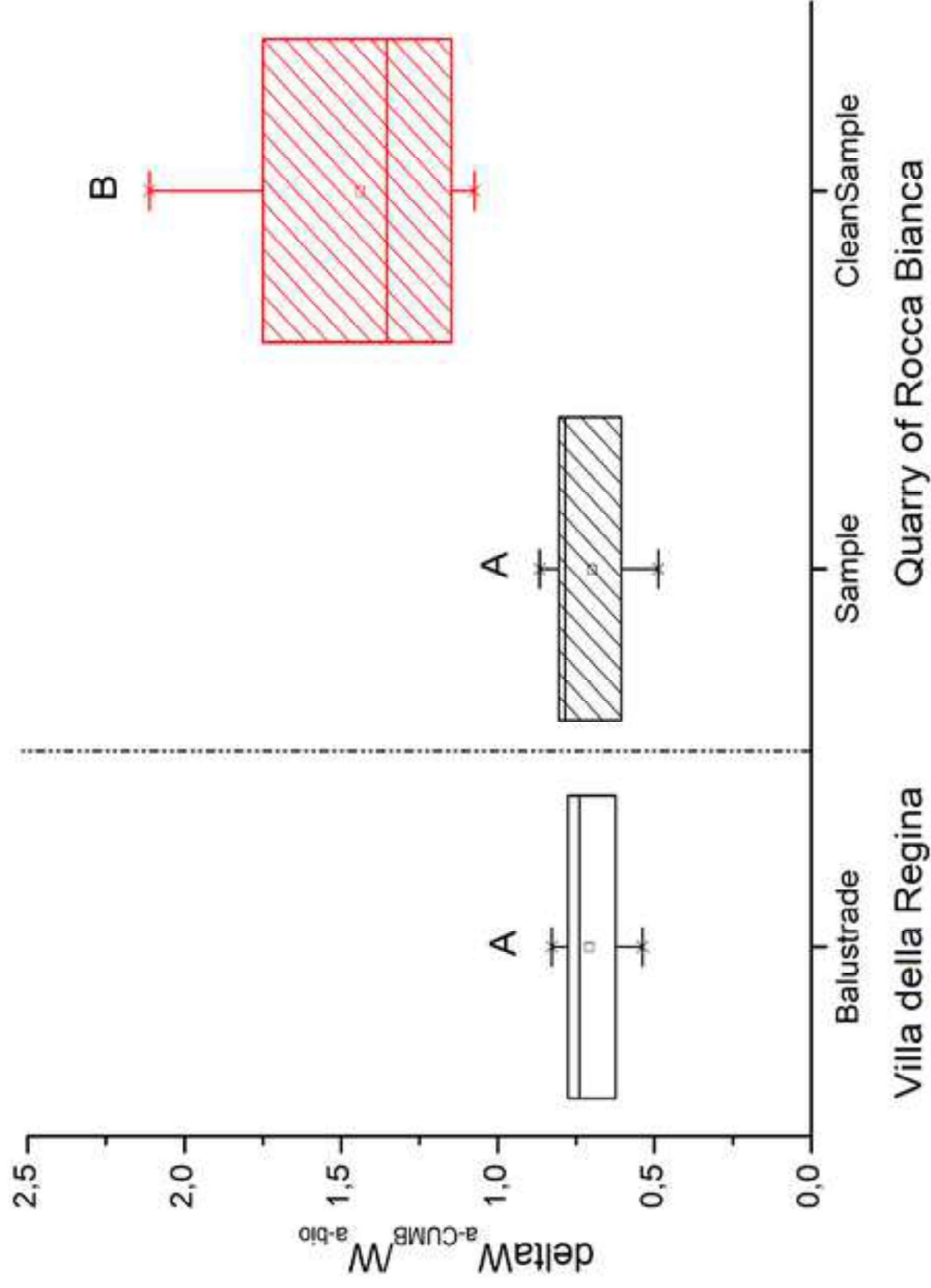
987 **Fig. 7.** Ordination of cross-sectioned samples prepared from blocks 1-6 of the Rocca Bianca
988 quarry on the basis of different parameters quantified by microscopic and UV observations
989 (A, axes 1 and 2; B, axes 1 and 3). Samples are marked according to different lithobionts
990 (biofilm, green symbols; *Staurothele areolate*, brown; *Pyrenodesmia erodens*, blue;
991 *Thelidium incavatum*, grey) and CUMBs (white), and blocks (1, diamond; 2, star; 3, square; 4,
992 down-triangle; 5, up-triangle; 6, circle). HD, hyphal penetration depth; DG, deep growths;
993 WL, white opalescent layer; DL, dark layer; WF, whitish, OF, orange, PF, pink, YF, yellow,
994 and BF, blue fluorescences.

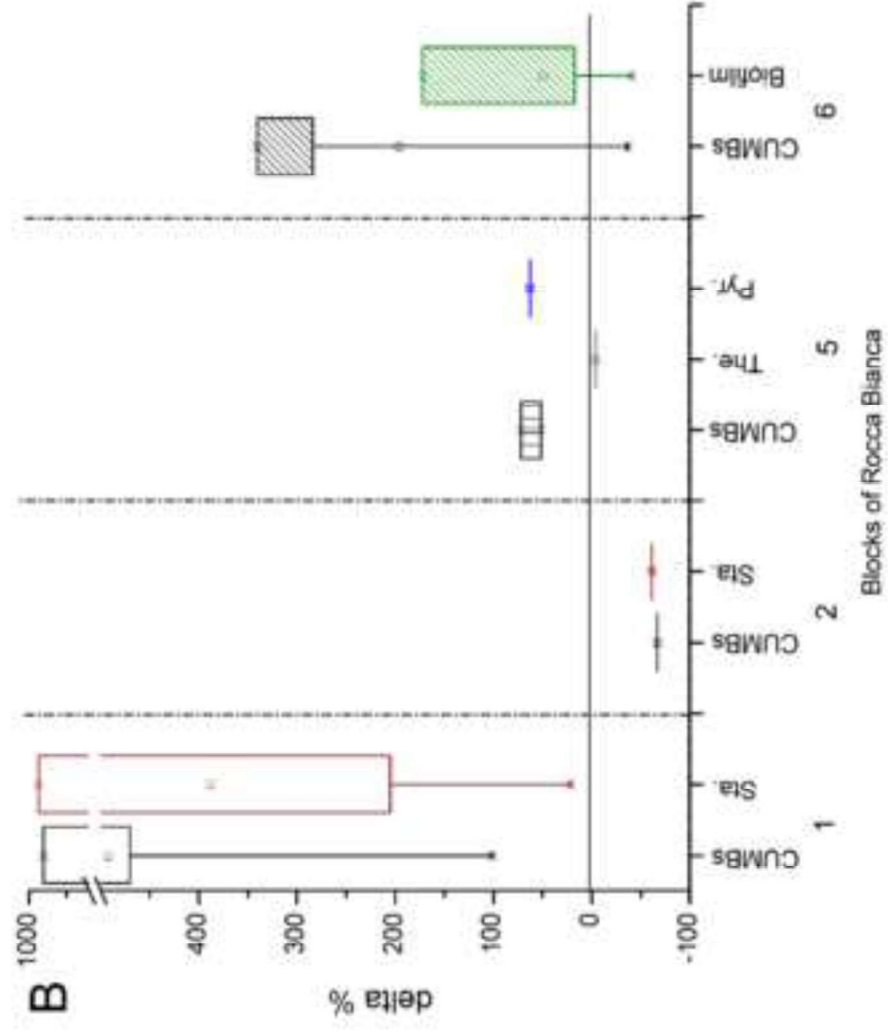
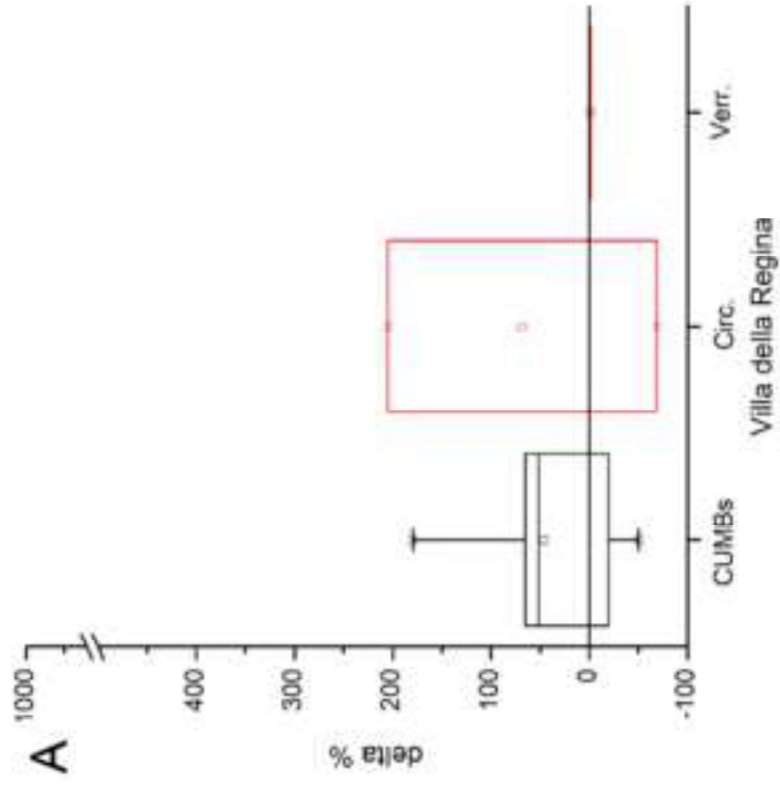


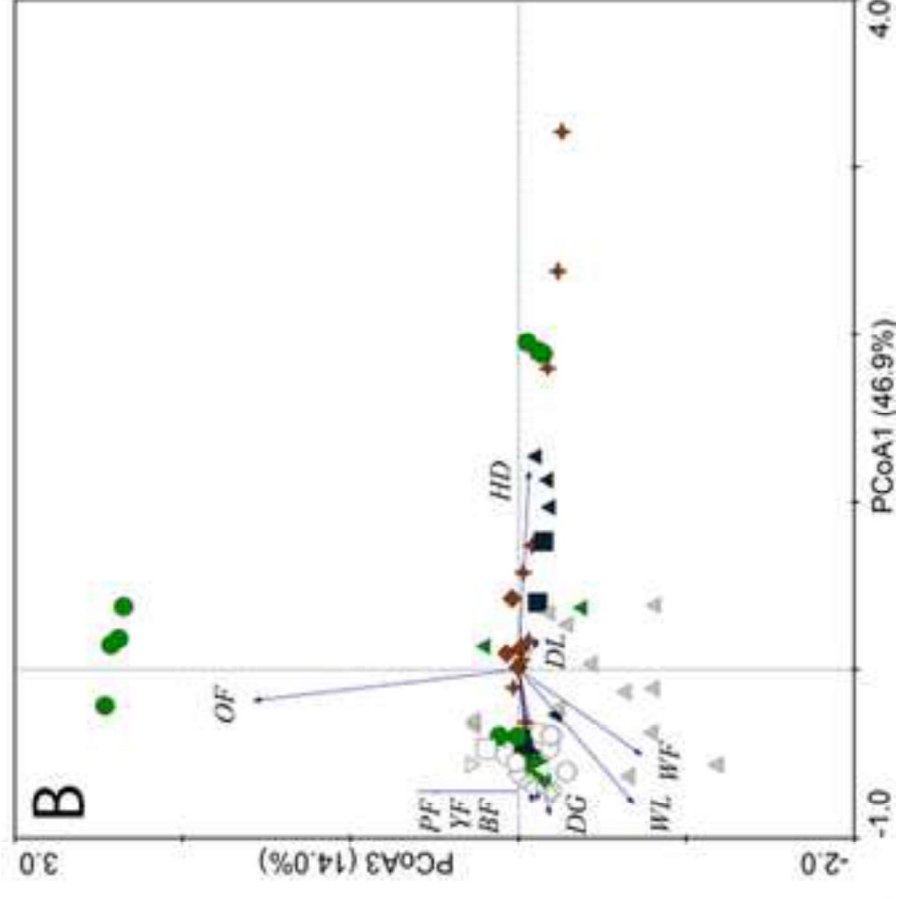
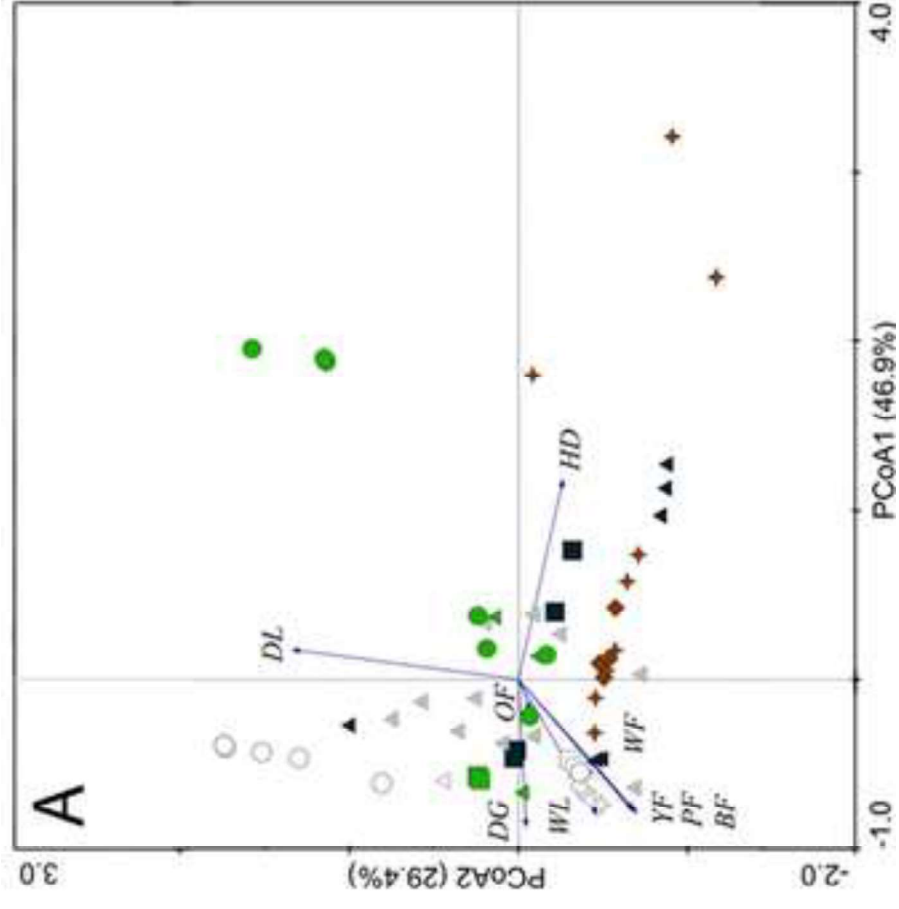








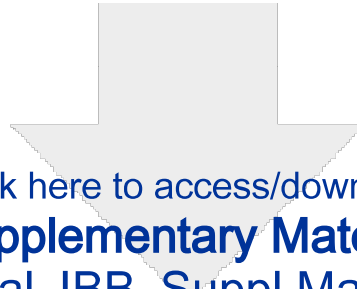




Declaration of interests

The authors declare that they have no known competing financial interests or personal relationships that could have appeared to influence the work reported in this paper.

The authors declare the following financial interests/personal relationships which may be considered as potential competing interests:



[Click here to access/download](#)

Supplementary Material

Cicardi et al_IBB_Suppl.Mat._def.docx

